Journal of Environmental Management 316 (2022) 115244

Contents lists available at ScienceDirect

Journal of Environmental Management

journal homepage: www.elsevier.com/locate/jenvman

Research article

# Snorkels enhance alkanes respiration at ambient and increased hydrostatic pressure (10 MPa) by either supporting the TCA cycle or limiting alternative routes for acetyl-CoA metabolism

Marta Barbato [a,b,1], Enza Palma [c,1], Ugo Marzocchi [d,e], Carolina Cruz Viggi [c], Simona Rossetti [c], Federico Aulenta [c,**], Alberto Scoma [a,b,*]

[a] Engineered Microbial Systems (EMS) Lab, Industrial Biotechnology Section, Department of Biological and Chemical Engineering (BCE), Aarhus University, Aarhus, Denmark
[b] Microbiology Section, Department of Biology, Aarhus University, Aarhus, Denmark
[c] Water Research Institute (IRSA), National Research Council (CNR), Monterotondo, Italy
[d] Center for Electromicrobiology, Section for Microbiology, Department of Biology, Aarhus University, Aarhus, Denmark
[e] Center for Water Technology WATEC, Department of Biology, Aarhus University, Aarhus, Denmark

ARTICLE INFO

*Keywords:*
Deep sea
Petroleum
Crude oil
Metatranscriptomics
BES
Oil spill

ABSTRACT

The impact of piezosensitive microorganisms is generally underestimated in the ecology of underwater environments exposed to increasing hydrostatic pressure (HP), including the biodegradation of crude oil components. Yet, no isolated pressure-loving (piezophile) microorganism grows optimally on hydrocarbons, and no isolated piezophile at all has a HP optimum <10 MPa (e.g. 1000 m below sea water level). Piezosensitive heterotrophs are thus largely accountable for oil clean up < 10 MPa, however, they are affected by such a mild HP increase in ways which are not completely clear. In a first study, the application of a bioelectrochemical system (called "oil-spill snorkel") enhanced the alkane oxidation capacity in sediments collected at surface water but tested up to 10 MPa. Here, the fingerprint left on transcript abundance was studied to explore which metabolic routes are 1) supported by snorkels application and 2) negatively impacted by HP increase. Transcript abundance was comparable for beta-oxidation across all treatments (also at a taxonomical level), while the metabolism of acetyl-CoA was highly impacted: at either 0.1 or 10 MPa, snorkels supported acetyl-CoA oxidation within the TCA cycle, while in negative controls using non-conductive rods several alternative routes for acetyl-CoA were stimulated (including those leading to internal carbon reserves e.g. 2,3 butanediol and dihydroxyacetone). In general, increased HP had opposite effects as compared to snorkels, thus indicating that snorkels could enhance hydrocarbons oxidation by alleviating in part the stressing effects imposed by increased HP on the anaerobic, respiratory electron transport chain. 16S rRNA gene analysis of sediments and biofilms on snorkels suggest a crosstalk between oil-degrading, sulfate-reducing microorganisms and sulfur oxidizers. In fact, no sulfur was deposited on snorkels, however, iron, aluminum and phosphorous were found to preferentially deposit on snorkels at 10 MPa. This data indicates that a passive BES such as the oil-spill snorkel can mitigate the stress imposed by increased HP on piezosensitive microorganisms (up to 10 MPa) without being subjected to passivation. An improved setup applying these principles can further support this deep-sea bioremediation strategy.

## 1. Introduction

Deep-sea life is featured by increased hydrostatic pressure (HP), which increases linearly with depth (~1 MPa/100 m in the water column; ~3 MPa/100 m in sediments (Oger and Jebbar, 2010)). Microorganisms adapted to increased HP have their maximum growth rate

* Corresponding author. Engineered Microbial Systems (EMS) Lab, Industrial Biotechnology Section, Department of Biological and Chemical Engineering (BCE), Aarhus University, Aarhus, Denmark.
** Corresponding author.
*E-mail addresses:* federico.aulenta@irsa.cnr.it (F. Aulenta), as@bce.au.dk (A. Scoma).
[1] These authors contributed equally to this work.

https://doi.org/10.1016/j.jenvman.2022.115244
Received 31 January 2022; Received in revised form 27 April 2022; Accepted 5 May 2022
Available online 20 May 2022

($\mu_{max}$) at HPs higher than surface water (0.1 MPa) and are called piezophiles, as opposed to piezosensitive microorganisms. The structural and metabolic traits resulting from high HP adaptation in piezophiles inhabiting the abysso- and hadopelagic zone (from 4000 m below seawater level [bswl], *i.e.* from 40 MPa) have historically been of great scientific interest (Abe, 2007; Kato et al., 1998; Seckbach et al., 2013; Simonato et al., 2006; Yayanos, 1995). What specific traits define microorganisms at milder HPs in epi- to bathypelagic waters (from surface up to 4000 m bswl) is less clear. This greatly limits our capacity to understand at which HP piezophiles begin to predominate over piezosensitive microorganisms and how much the latter contribute to underwater nutrients cycling. For instance, ever since their discovery 40 years ago (Yayanos et al., 1979), no piezophile has been isolated with a HP optimum <10 MPa (Scoma, 2021). This suggests that piezosensitive microorganisms are relevant but neglected players in the microbial ecology and biogeochemistry of waters and sediments <10 MPa (e.g. from surface to 1000 m bswl). The lack of microorganisms that grow optimally between 0.1 and 10 MPa is of particular concern for petroleum-contaminated underwater environments, as oil spills most commonly concern areas exposed to these mild HPs (NOAA/Hazardous Materials Response and Assessment Division Seattle, 1992). Since there is currently no isolated piezophile which requires hydrocarbons as sole carbon source to express piezophily (Scoma, 2021), this concern extends to cases such as the relatively recent British Petroleum spill at the Deepwater Horizon in the Gulf of Mexico in 2010 which originated at ~15 MPa (reviewed in (Joye et al., 2014; Kimes et al., 2014; King et al., 2015; Scoma et al., 2016c)). The closest exception is the recently isolated *Alcanivorax venustensis* R-72943, the growth rate of which is still affected- albeit not dramatically- at 10 as compared to 0.1 MPa (at 20 °C (Van Landuyt et al., 2020)). Hence, piezosensitive heterotrophs, including those growing primarily on hydrocarbons (the so-called obligate oil degraders), appear to be majorly accountable for oil bioremediation up to 10 MPa. Yet, they do suffer from a mild HP increase. Microbial communities collected up to 1000 bswl (thus theoretically adapted at least in part to *in situ* HPs up to 10 MPa) were repeatedly shown to suffer a reduction of 5–10% of their oil degradation capacity for every 1 MPa increase (Marietou et al., 2018; Nguyen et al., 2018; Scoma et al., 2018). Deep-sea bioremediation technologies working with petroleum-contaminated areas experiencing up to 10 MPa must thus find strategies to alleviate the negative HP effects on piezosensitive microorganisms. Most of the literature on the HP effects on oil biodegradation focuses on microbial community assembly (Barbato and Scoma, 2020; Fasca et al., 2017; Gontikaki et al., 2018; Marietou et al., 2018; Noirungsee et al., 2020; Perez Calderon et al., 2019; Potts et al., 2018; Van Landuyt et al., 2020), with the few studies on cell metabolism reported by this group (transcriptomics in pure cultures (Scoma et al., 2016a; Scoma et al., 2016b) or meta-proteomics in mixed cultures (Scoma et al., 2018)). In general, the latter suggest that increased HP likely forces cells to use increasingly more energy for cell maintenance rather than growth. However, a much deeper understanding is required before technological solution can be applied to enhance microbial oil metabolism underwater.

In a previous study ((Aulenta et al., 2021); Fig S2,S3) we reported on an enhanced oil bioremediation at increased HP using an electrochemical system (snorkels, in the following). Microbial communities in pristine sediments collected at 30 m bswl were supplied with crude oil and subjected to ambient and increased HP (0.1 and 10 MPa). Reactors were provided with either 1) non-polarized electrodes (snorkels) bridging contaminated sediments with overlaying seawater; or 2) non-conductive glass rods (used as negative controls) (experimental set up in Fig. S1). Snorkels are electrically-conductive graphite rods not connected to electrical power. The lower portion of the rod is inserted in contaminated sediments and acts as an anode, while the upper portion is in contact with oxygen in overlying waters and functions as a cathode. Electrons derived from the microbial oxidation of contaminants and other reduced organic and inorganic species travel through this graphite electrode to reduce oxygen in the upper aerobic portion of the rod, thereby forming water (Viggi et al., 2015, 2017). Snorkels were shown to enhance oil bioremediation at ambient pressure ((Mapelli et al., 2017; Marzocchi et al., 2020; Matturro et al., 2017; Viggi et al., 2017; Viggi et al., 2015)), although the exact implications for microbial metabolism were not completely elucidated. Our experiments tested two crude oils, carrying either a high or a low concentration of alkanes (15 vs. 4%, Statfjord vs. DUC oil). In particular, in (Aulenta et al., 2021) we reported that when using the alkane-rich crude oil: A) the application of snorkels enhanced alkanes oxidation at both 0.1 and 10 MPa within only 7 weeks with respect to (wrt) glass controls (Fig. S2D); B) at 0.1 MPa, snorkels enhanced the removal of total petroleum hydrocarbons (TPH) wrt to glass controls (Fig. S2B); C) less TPH were removed at 10 wrt 0.1 MPa despite the application of snorkels (Fig. S2B). Besides, with either crude oil and HP, the application of snorkels left a clear fingerprint on the cycling of sulfur species in sediments (Fig. S3A-F), and a less evident fingerprint on the oxygen concentration in overlying seawaters (Fig. S3H).

The present study aims to further elucidate snorkels fingerprint on oil bioremediation at increased HP when this was most improved (i.e. when using the alkane-rich [15%] Statfjord-oil-contaminated sediments), by focusing on: 1) microbial gene expression in sediments; 2) microbial community assemblage in sediments and in biofilms on the snorkels surface; 3) iron cycling in sediments; and 4) elemental composition on the snorkels surface. To support relevant observations on point 2 to 4, sediments and snorkels incubated with the alkane-poor (4%) DUC oil were used as controls.

## 2. Materials and methods

### 2.1. Sediment sampling and reactor configuration

All information in (Aulenta et al., 2021). Briefly, sediment samples were collected from Aarhus Bay (Denmark) at 30 m bswl. The upper 10–12 cm of sediment was discarded to exclude large burrowing animals, with the remaining sieved (mesh 0.5 mm) to remove solid residues. This pristine sediment was then contaminated in the lab with either Statfjord or DUC oil to a final concentration of 1% (v:w) as in (Viggi et al., 2015).

Bioelectrochemical oil remediation was assessed in glass cylinders with either conductive graphite rods (snorkels) or non-conductive glass rods (negative controls), and applying either ambient or increased HP (0.1 or 10 MPa). The treatments tested: snorkels at increased HP (HPS); glass controls at increased HP (HPC); snorkels at ambient pressure (APS); and glass controls at ambient pressure (APC) (Fig. S1). Graphite and glass rods were inserted into the sediment for 8 cm, with the remaining 7 cm above the sediment surface. In each cylinder, the two rods were connected at the top by a carbon felt disc to extend the cathodic surface (also in negative controls). Glass cylinders were filled with 200 mL of sterile, artificial seawater, which was oxygenated at the beginning of the experiment (no gas phase was left). Cylinders were place in the dark at 14 ± 2 °C. At 10 MPa, cylinders were placed in a 5-L high-pressure reactor. HP was changed manually via a HP pump (Enerpac, Netherlands) following compression/decompression rates as in (Scoma et al., 2019). Experiments were conducted in three independent replicates.

### 2.2. Metatranscriptomic analysis

#### 2.2.1. Sediment sampling and storage

Sediment samples (two biological replicates for each experimental group) were collected, immediately frozen with liquid nitrogen and stored at −80 °C until RNA extraction.

#### 2.2.2. RNA extraction and quantification

RNA was extracted from 2 g of sediments with the RNeasy®

PowerSoil® Total RNA Kit (QIAGEN) following the manufacturer's instructions. Co-extracted DNA was depleted with the DNAse TURBO DNA-free™ Kit (Thermo Fisher Scientific, Waltham, MA, USA). The RNA concentration was measured in duplicate using the Qubit HS RNA assay kit (Thermo Fisher Scientific, Waltham, MA, USA) and DNA contamination was evaluated with the Qubit™ dsDNA HS (Thermo Fisher Scientific, Waltham, MA, USA). Extracted RNA samples were stored at −80 °C before being submitted to DNASense ApS (Aalborg, Denmark) for sequencing.

#### 2.2.3. RNA quality, cDNA synthesis and illumina sequencing

Prior to cDNA synthesis, RNA quality and integrity were confirmed for selected samples using 4200 TapeStation with RNA ScreenTape (Agilent Technologies). DNASense ApS received the extracted RNA and prepared the samples for sequencing using the NEB Next Ultra II RNA library preparation kit (New England Biolabs) according to the manufacturer's instructions. Library concentrations were measured using Qubit HS DNA assay and library size estimated using TapeStation D1000 ScreenTapes (Agilent Technologies). The samples were pooled in equimolar concentrations and paired-end sequenced (2 × 150 bp) on a HiSeq X (Illumina, USA).

#### 2.2.4. Processing of metatranscriptome data

Sequencing read quality was assessed through the FastQC quality control pipeline Version 0.11.9 (Andrews, 2010). Reads were trimmed and quality-filtered with the Trimmomatic tool version 0.39 (CROP:150, HEADCROP:10, SLIDINGWINDOW = 4:30, MINLEN = 50; ILLUMINACLIP function was used to remove the adapters sequences) (Bolger et al., 2014). Sequences were dereplicated with the BBtools/dedupe. sh tool (maxsubs = 0 int = t ac = f) and putative mRNA sequences were separated from ribosomal RNA sequences with SortMeRNA v2.1 which mapped all reads to the ribosome RNA databases: SILVA arc 16S, arc 23S, bac 16S, bac 23S, euk 18S, euk 28S; RFAM 5S, 5.8S (Kopylova et al., 2012). Only the putative mRNA reads were used for subsequent analysis. To increase efficiency of annotation, mRNA reads were *de novo* assembled with rnaSPAdes v3.14.1 (Antipov et al., 2019; Bushmanova et al., 2019; Korobeynikov, 2019) using default settings. Genes were predicted with FragGeneScan (Rho et al., 2010) using default parameters. Function and taxonomy of the reconstructed genes was annotated with EggNOG mapper v2 (Cantalapiedra et al., 2021; Huerta-Cepas et al., 2019) and GhostKOALA v 2.2 (from the database Kyoto Encyclopedia of Genes and Genomes - KEGG) (Kanehisa et al., 2016).

Reads were mapped on the *de novo* reconstructed contigs with the BBtools/bbmap. sh tool with default parameter and the pileup. sh tool was used to retrieve the abundance (fragments per kilobase per million mapped, fpkm) of each read from the file created by bbmap.

#### 2.2.5. Analysis of differential gene expression

Two biological replicates were analyzed per each treatment (HPS, HPC, APS, APC). The fpkm of each read that corresponded to the same gene (based on the annotation procedure) were summed to have the total abundance of each gene transcript. The transcription level of each gene was investigated also at the taxonomical level, with the taxonomical affiliation obtained after the gene annotation with both EggNOG mapper v 2 and GhostKOALA v 2.2. We calculated the fpkm average values and standard deviation for each sample group of each gene and taxonomical group associated to each gene. Comparison among different groups was performed with student T-test and log2 fold change ($log2_{fc}$). T-test was calculated with the Calc Statistical Function of Microsoft$^{R}$ Office. Transcription level was considered significative if $P \leq 0.05$ and $log2_{fc}$ was used to determine higher/lower transcript abundance.

#### 2.2.6. Accession numbers

The raw sequencing reads are available in the Sequence Read Archive (SRA) NCBI within the BioProject accession number PRJNA787061, BioSample number SAMN23768613 under the accession numbers SRR17165215-SRR17165222.

### 2.3. Analysis of the 16 S rRNA gene amplicon in sediments and snorkels biofilm

DNA extraction and 16S rRNA gene amplicon sequencing were conducted as in (Marzocchi et al., 2020) on one sample per condition. Concerning the biofilms on snorkels, they were collected by gently scratching the snorkel surface with a sterile knife (~1 g of material).

### 2.4. X-ray photoelectron spectroscopy (XPS)

The surface chemical composition of graphite rods was determined using one sample per condition. Measurements were performed in an Escalab 250Xi spectrometer (Thermo Fisher Scientific, UK) equipped with a monochromatic Al Kα source and a 6-channeltron detection system. The photoemission spectra were collected at the base pressure of 5 × 10-8 Pa, by using 40 eV pass energy of the analyzer and standard electromagnetic lens mode with ~1 mm diameter of analyzed area. Spectroscopic data were processed with Avantage v.5 software. Shirley background and mixed Lorentzian/Gaussian peak shape (30%) with linked peak widths were used for the peak fitting.

### 2.5. Chemical analysis

$Fe^{2+}$ was determined using the Ferrozine method (Stookey, 1070). Acid volatile sulfur (AVS) was determined on a wet sample after acidification as in (Yücel et al., 2010). High-resolution depth profiles of pH were recorded with micro-electrodes built at Aarhus University, and conducted as described in (Marzocchi et al., 2020). Total petroleum hydrocarbons (TPH) and *n*-alkanes were measured as in (Aulenta et al., 2021).

### 2.6. Statistical analysis

Chemical analysis results were expressed as mean values of three independent biological replicates. Bars in the graphs indicated standard deviation (st. dev.). Significant differences were analyzed with the Calc Statistical Function of Microsoft$^{R}$ Office applying student T-test. Differences were considered significative if $P \leq 0.05$.

## 3. Results

### 3.1. General overview of the meta-transcriptomic data

Gene expression in the alkane-rich (15%), Statfjord-oil-contaminated sediments was analyzed (Figs. 1–6; Fig. S4-S28). 112,995 gene transcripts were annotated (52.05% of the predicted genes), with the most diverse gene expression (i.e. transcripts in at least 200 pathways, based on KEGG KO numbers) related to: carbohydrate, amino acid, energy, cofactors and vitamins and lipid metabolism (Table S1A-F; Fig. S4-S8). Within the xenobiotics biodegradation (Fig. 1), transcript abundance was highest (≥500 fpkm per sample) for the pathways: nitrotoluene, benzoate, naphthalene, chloroalkane and chloroalkene degradation, and drug metabolism and other enzymes (Fig. 1). In general, the increase in HP had no effect or significantly decreased ($P < 0.05$) transcript abundance in otherwise similar sediments (i.e. HPS *vs.* APS; or HPC *vs.* APC) (namely in: toluene, polycyclyc aromatic hydrocarbon, nitrotoluene, naphthalene, chloroalkane and chloroalkene, caprolactam and benzoate degradation; Fig. 1). On the other hand, application of snorkels rather than glass controls had a different impact depending on HP: at ambient pressure (APS *vs.* APC), snorkels enhanced the transcript abundance in benzoate, caprolactam, polycyclyc aromatic hydrocarbons and toluene degradation; at increased pressure (HPS *vs.* HPC), snorkels decreased the transcript

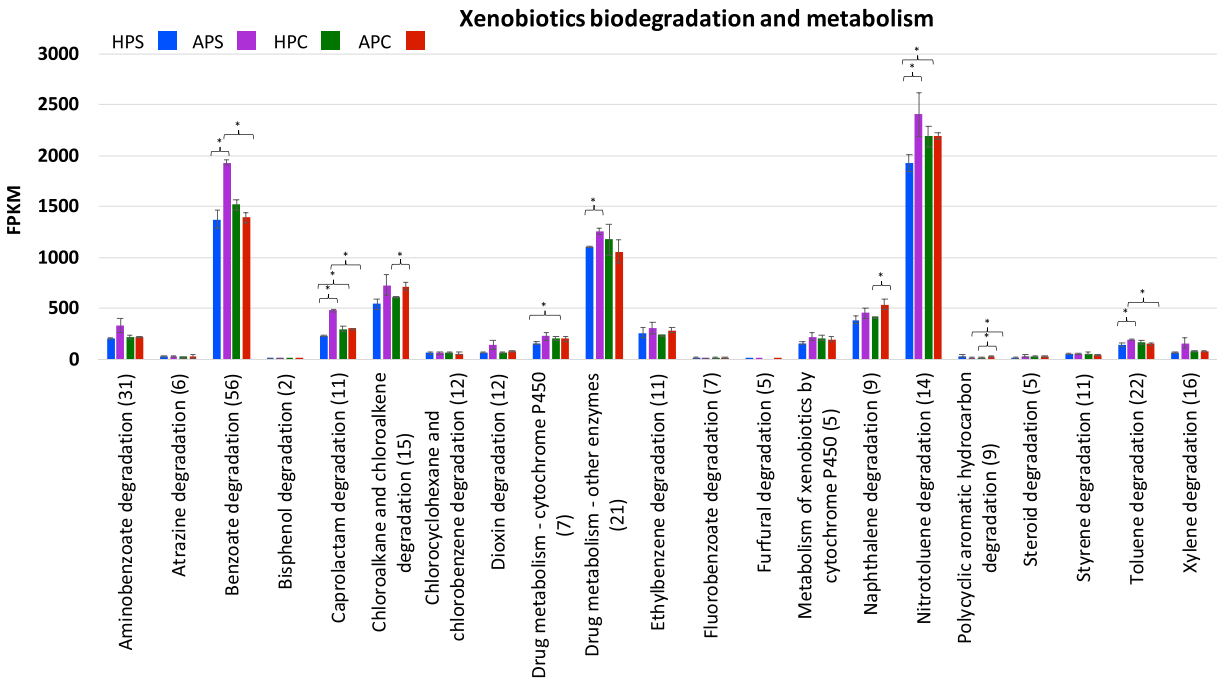


**Fig. 1.** Expression of genes in the Xenobiotics biodegradation and metabolism pathway (see KEGG database, https://www.genome.jp/kegg/) at the end of 7 weeks of incubation in sediments contaminated with Statfjord oil, in each of the treatment tested in the present study. Keys presented in the graph. Brackets and asterisks indicate statistically different levels of expression. (For interpretation of the references to color in this figure legend, the reader is referred to the Web version of this article.)

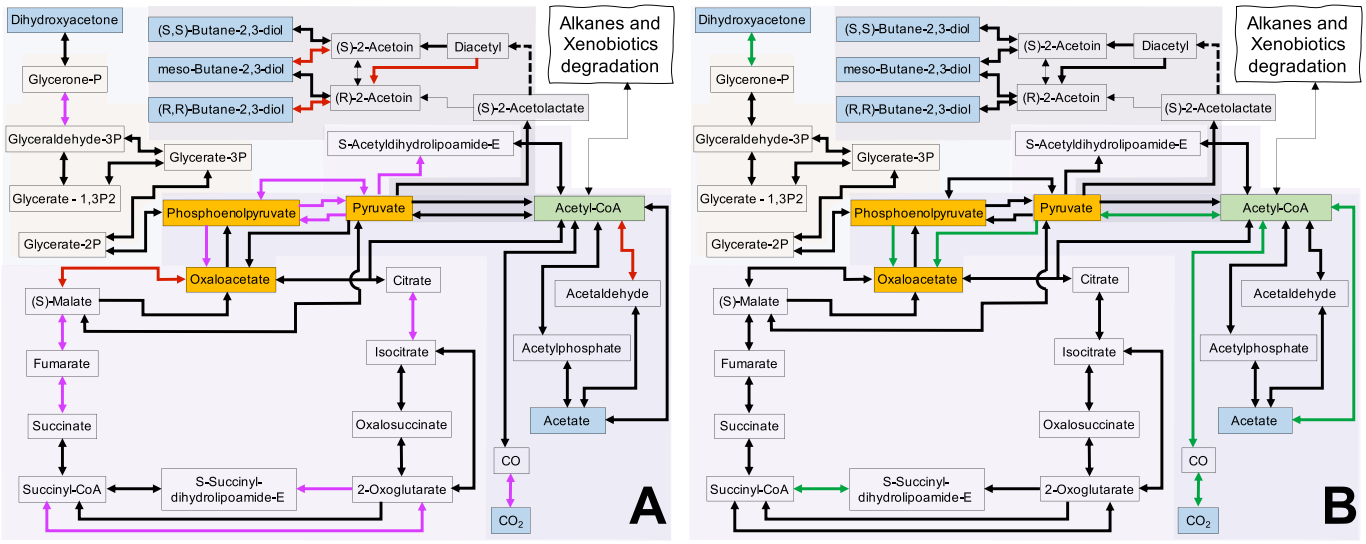


**Fig. 2.** Expression of genes in selected pathways of the Carbohydrate Metabolism and other pathways related to them (i.e., gluconeogenesis, and pyruvate, butanoate and methane metabolism; KEGG database, https://www.genome.jp/kegg/) at the end of 7 weeks of incubation in sediments contaminated with Statfjord oil, in APS and APC. Molecules which are enzymatically converted between one another are connected by arrows (multiple arrows between the same two boxes indicate different enzymes, see also KEGG database). Thin arrows indicate that the enzyme exists, but was not expressed in either APS or APC. Dotted lines indicate that the reaction is not enzymatic. Bold arrows in either black, red or purple indicate expression of the enzyme. In particular, purple arrows indicate an upregulation in APS, while arrows in red upregulation in APC. Up- or down-regulation refer to statistically different levels of expression. (For interpretation of the references to color in this figure legend, the reader is referred to the Web version of this article.)

abundance in nitrotoluene and caprolactam degradation, and drug metabolism and cytochrome P450 (Fig. 1).

### 3.2. *Alkanes activation and beta oxidation*

Application of snorkels to contaminated sediments at ambient pressure (APS *vs.* APC) significantly enhanced both TPH ($C/C_0$, 0.64 ± 0.04 vs. 1.03 ± 0.07, Fig. S2B) and alkanes biodegradation ($C/C_0$, 0.65 ± 0.01 vs. 0.89 ± 0.02, Fig. S2D). Microbial alkane degradation initiates with the activation of alkanes into fatty acids, which then enter *beta* oxidation to form acetyl-CoA. Transcript abundance for alkanes activation and *beta* oxidation pathway was however comparable among all treatments (Fig. S9), each enzyme expressed by the main taxa essentially in a comparable way ($P > 0.05$; Fig. S10-S22). The observed difference in

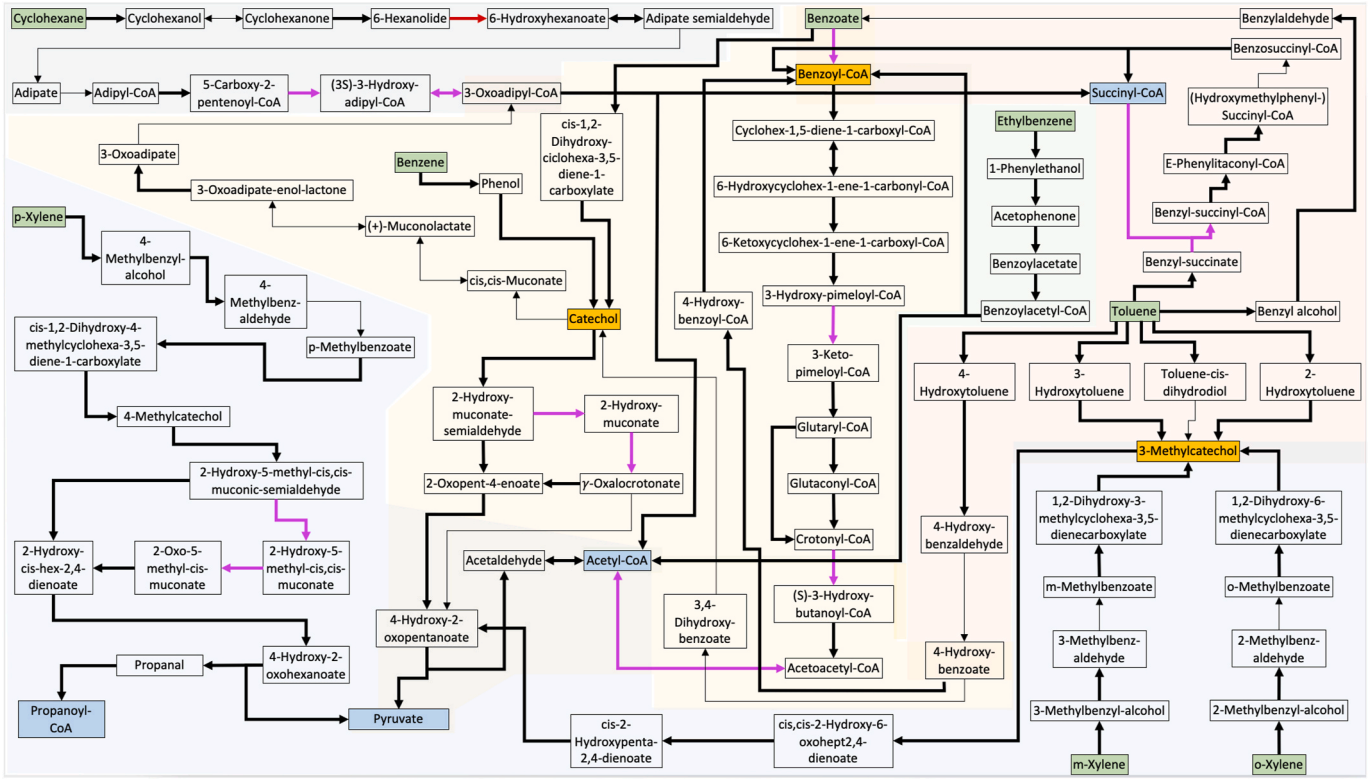


**Fig. 3.** Expression of genes in Xenobiotics metabolism (namely, benzoate, toluene, xylene, caprolactam [ciclohexane] and ethylbenzene; KEGG database, https://www.genome.jp/kegg/) at the end of 7 weeks of incubation in sediments contaminated with Statfjord oil, in APS and APC. Molecules which are enzymatically converted between one another are connected by arrows (multiple arrows between the same two boxes indicate different enzymes, see also KEGG database, https://www.genome.jp/kegg/). Thin arrows indicate that the enzyme exists, but was not expressed in either APS or APC. Bold arrows in either black, red or purple indicate expression of the enzyme. In particular, purple arrows indicate an upregulation in APS, while arrows in red upregulation in APC. Up- or down-regulation refer to statistically different levels of expression. (For interpretation of the references to color in this figure legend, the reader is referred to the Web version of this article.)

biodegradation may thus have depended on other metabolic pathways. The most recurrently impacted were: 1, carbohydrate metabolism (and the related pathways gluconeogenesis, and pyruvate, butanoate and methane metabolism); 2, xenobiotics biodegradation; and 3, energy metabolism (i.e. nitrogen and sulfur). The effects of either snorkel application or HP increase on such pathways is discussed hereafter (additional data in the Supplementary Information).

### 3.3. The impact of snorkels on gene expression

#### 3.3.1. At ambient pressure (APS vs. APC)

*3.3.1.1. Carbohydrate metabolism.* Application of snorkels in APS enhanced the transcript abundance of several genes in the TCA cycle wrt APC (Fig. 2A; Table S2,S3B), likely to support the high rate of acetyl-CoA generated after hydrocarbons oxidation. This is in agreement with the higher crude oil biodegradation (both alkanes and TPH) in APS wrt APC (Fig. S2B,D), and with the higher transcript abundance for alternative pathways processing acetyl-CoA in APC, namely, the conversion of diacetyl to 2,3 butanediol (K00004; $P = 0.004$, log2 fold change ($log2_{fc}$) = 1.17, fpkm = 12 vs. 5; Table S2). K00004 was mainly expressed by *Clostridia* (50–35% of all fpkm, in APC and APS, respectively; Table S3J), and by *Alphaproteobacteria* (solely present in APC, ~30% of all fpkm, $P = 0.022$; Table S3J).

*3.3.1.2. Xenobiotics biodegradation and metabolism.* The most impacted xenobiotics biodegradation pathways in all treatments were benzoate, toluene, xylene, caprolactam (ciclohexane) and ethylbenzene (green boxes in Fig. 3). These are interconnected through some key intermediates (e.g. benzoyl-CoA, catechol, 3-methylcatechol, orange boxes in Fig. 3) and lead to common products (i.e. pyruvate, and acetyl-, succinyl- and propanoyl-CoA, blue boxes in Fig. 3). There was only a negligible difference in the transcript abundance for xenobiotics biodegradation in APS wrt APC. In the benzoate degradation pathway, the transcript abundance in the benzoyl-CoA conversion to, eventually, acetyl-CoA entering the TCA cycle was higher in APS (in 4/15 genes; Fig. 3, Table S2,S3E). In the xylene degradation pathway, 12/14 genes for the conversion of *p*-xylene to propanoyl-CoA were annotated and just 2/14 had higher transcript levels in APS (Fig. 3, Table S2,S3E). Within propanoate metabolism (KEGG map 00640), propanoyl-CoA can be converted into acetyl-CoA (e.g. via 3-oxopropionyl-CoA; 4/7 genes annotated, 1/7 with higher transcript levels in APS) or to succinyl-CoA (e.g. via (R)-methyl-malonyl-CoA, 3/3 genes annotated) (Table S2,S3G), both products being intermediates of the TCA cycle (Fig. 2A). Notwithstanding these minor differences, TPH removal was higher in APS wrt APC (Fig. S2B). As for alkanes activation and *beta* oxidation, this suggests that the major impediment to a comparable TPH removal in APS and APC was likely due to processes related to xenobiotics metabolism, as for instance the TCA cycle which uses several of its products (e.g. pyruvate, and acetyl- and succinyl-CoA; Fig. 2A).

#### 3.3.2. At increased pressure (HPS vs. HPC)

*3.3.2.1. Carbohydrate metabolism.* None of the TCA cycle genes was impacted at increased HP by the application of snorkels wrt glass controls (Fig. 2B, Table S4,S5A-K). However, a higher transcript abundance in HPC wrt HPS was found for two alternative pathways processing acetyl-CoA: one leading to its conversion to acetate (K01895; $P = 0.016$, $log2_{fc} = 0.35$, fpkm = 404 vs. 317; Table S4,S5K); and another to carbon monoxide (CO) and eventually carbon dioxide ($CO_2$) (namely, K00194,

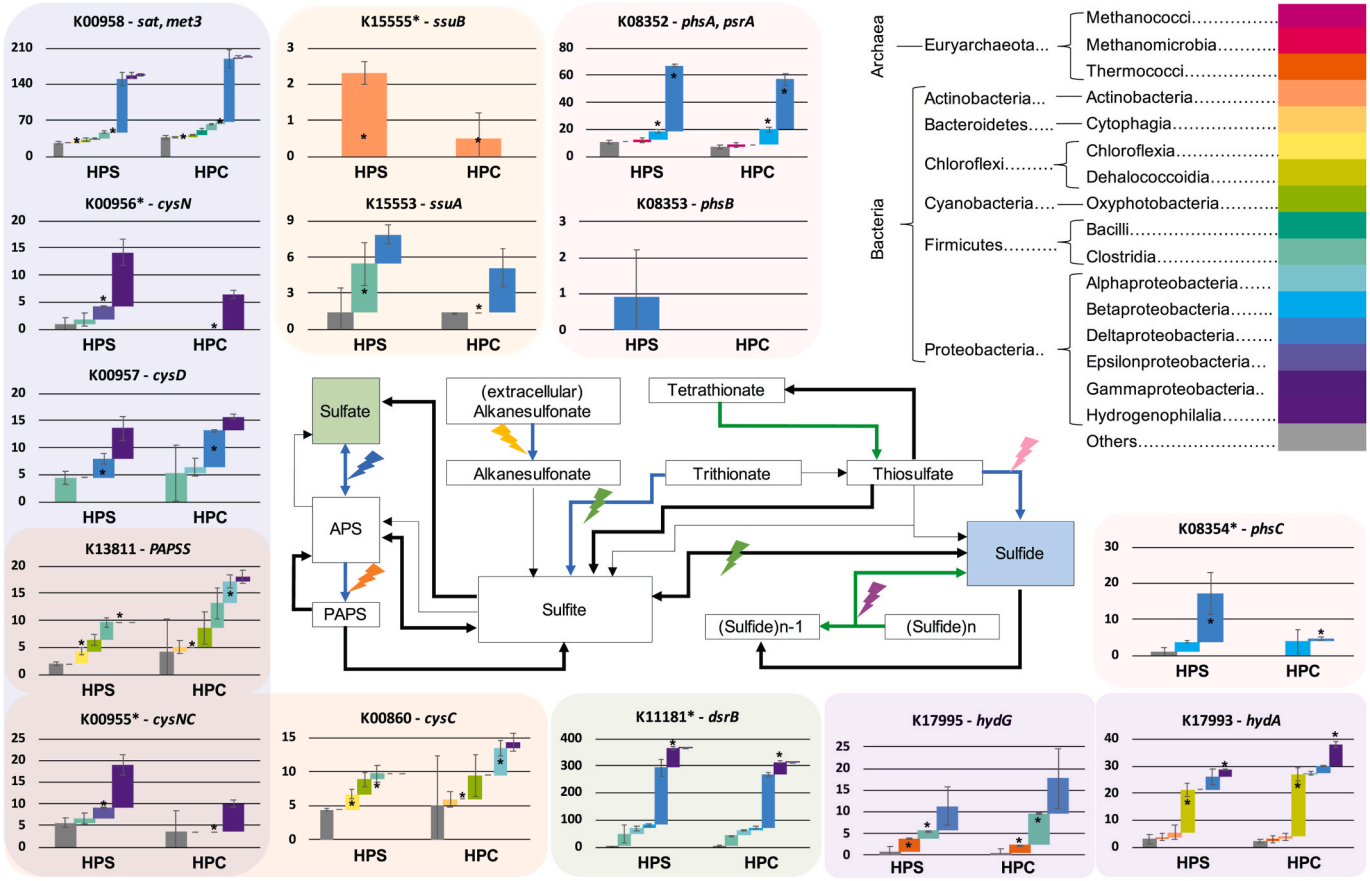


**Fig. 4.** Expression of genes in sulfur metabolism (KEGG database, https://www.genome.jp/kegg/) and their taxonomical composition at the end of 7 weeks of incubation in sediments contaminated with Statfjord oil, in HPS and HPC. Molecules which are enzymatically converted between one another are connected by arrows (multiple arrows between the same two boxes indicate different enzymes, see also KEGG database). Thin arrows indicate that the enzyme exists, but was not expressed in either HPS or HPC. Bold arrows in either black, blue or green indicate expression of the enzyme. In particular, blue arrows indicate an upregulation in HPS, while arrows in green upregulation in HPC. Up- or down-regulation refer to statistically different levels of expression. Concerning taxonomy, the lightning symbols on some arrows relate to the taxonomical distribution of the annotated sequences: the color of the lightning corresponds to that of the box where bar charts with taxonomical distributions are reported. Asterisks on top of bars indicate significant difference between the HPS and HPC for that specific taxa. Keys for the bar charts are reported in the figure, upper right. (For interpretation of the references to color in this figure legend, the reader is referred to the Web version of this article.)

$P = 0.018$, $\log2_{fc} = 0.49$, fpkm = 168 vs. 120; and K00198, P = 0.024, $\log2_{fc} = 0.21$, fpkm = 475 vs. 410; Table S4,S5K), providing reducing power in the form of reduced ferredoxin. In particular, in HPC acetyl-CoA conversion to acetate (K01895) was primarily due to *Deltaproteobacteria* (>45% of all fpkm, $P = 0.006$; Table S5K), while acetyl-CoA conversion to $CO_2$ (K00194, K00198) was primarily due to *Deltaproteobacteria* and *Clostridia* (>57% and 19% of all fpkm, respectively, $P < 0.046$; Table S5K). Last, acetyl-CoA may have been used for the intracellular accumulation of dihydroxyacetone, with higher transcript levels for several genes involved in just 2/7 conversion steps (at the beginning and end of the pathway; K00169, K00172, K00171, K00189 and K00863; Fig. 2B, Table S4). In all such transcripts, *Clostridia* represented the most abundant taxa (generally 20–30% of all fpkm; Table S5B,K). The fact that alternative pathways to the TCA cycle to process acetyl-CoA had higher transcript levels in the absence of the snorkel (here, HPC wrt HPS) is in agreement with what observed in APC wrt APS with 2,3 butanediol generation (Fig. 2A).

*3.3.2.2. Energy metabolism: sulfur.* $SO_4^{2-}$ was a primary electron acceptor in oil-contaminated marine sediments (Fig. S3E,F). In the assimilatory pathway, $SO_4^{2-}$ is part of an energy-consuming metabolism that eventually produces sulfur compounds and leads to the biosynthesis of sulfur-containing amino acids. In the dissimilatory pathway, energy is produced while $SO_4^{2-}$ is reduced to form sulfide ($H_2S$). In our set up, $H_2S$ could be oxidized by snorkels (Fig. S3A-D) to form oxidized forms of sulfur (e.g. $SO_4^{2-}$; Fig S3E,F), as opposed to non-conductive glass controls were $H_2S$ accumulated (Fig. S3A-D).

Transcript abundance in the dissimilatory pathway was much higher wrt the assimilatory, for both HPS and HPC ($P \leq 0.009$, $1.26 < \log2_{fc} < 1.82$; Table S6A,B). However, transcripts related to the energy-consuming assimilatory pathway were more abundant in HPC wrt HPS ($P = 0.038$, $\log2_{fc} = 0.62$, 699 vs. 454; Table S6A,B). This means that the application of snorkels did not favor the energy-consuming assimilatory pathways at increased HP (HPS vs. HPC). Overall, the most abundant microbial classes involved in $SO_4^{2-}$ metabolism were comparable in HPS and HPC (i.e. *Deltaproteobacteria*, *Gammaproteobacteria* and *Clostridia*, Fig. S23), however, in HPS some specific taxa were significantly more active on the assimilatory rather than dissimilatory pathway (i.e. *Chloroflexi* and *Epsilonproteobacteria*). Several transcripts in the assimilatory pathway related to the activation of $SO_4^{2-}$ by reaction with ATP to form adenylyl $SO_4^{2-}$ (K00955, K00956) and the subsequent adenylyl $SO_4^{2-}$ conversion to 3′-phosphoadenylyl $SO_4^{2-}$ (PAPS) (K00955) were more abundant in HPS wrt HPC (Fig. 4, Table S5D). In particular, transcripts from *Chloroflexia* (K13811, K00860 and to a minor extent K00958) and *Epsilonproteobacteria* (K00955, K00956) were solely found in HPS (Fig. 4, Table S5D). The following conversion of PAPS into sulfite ($SO_3^{2-}$) within the assimilatory $SO_4^{2-}$ pathway (K00390) had comparable levels in HPS and HPC ($P > 0.05$, Table S4), however, transcripts from

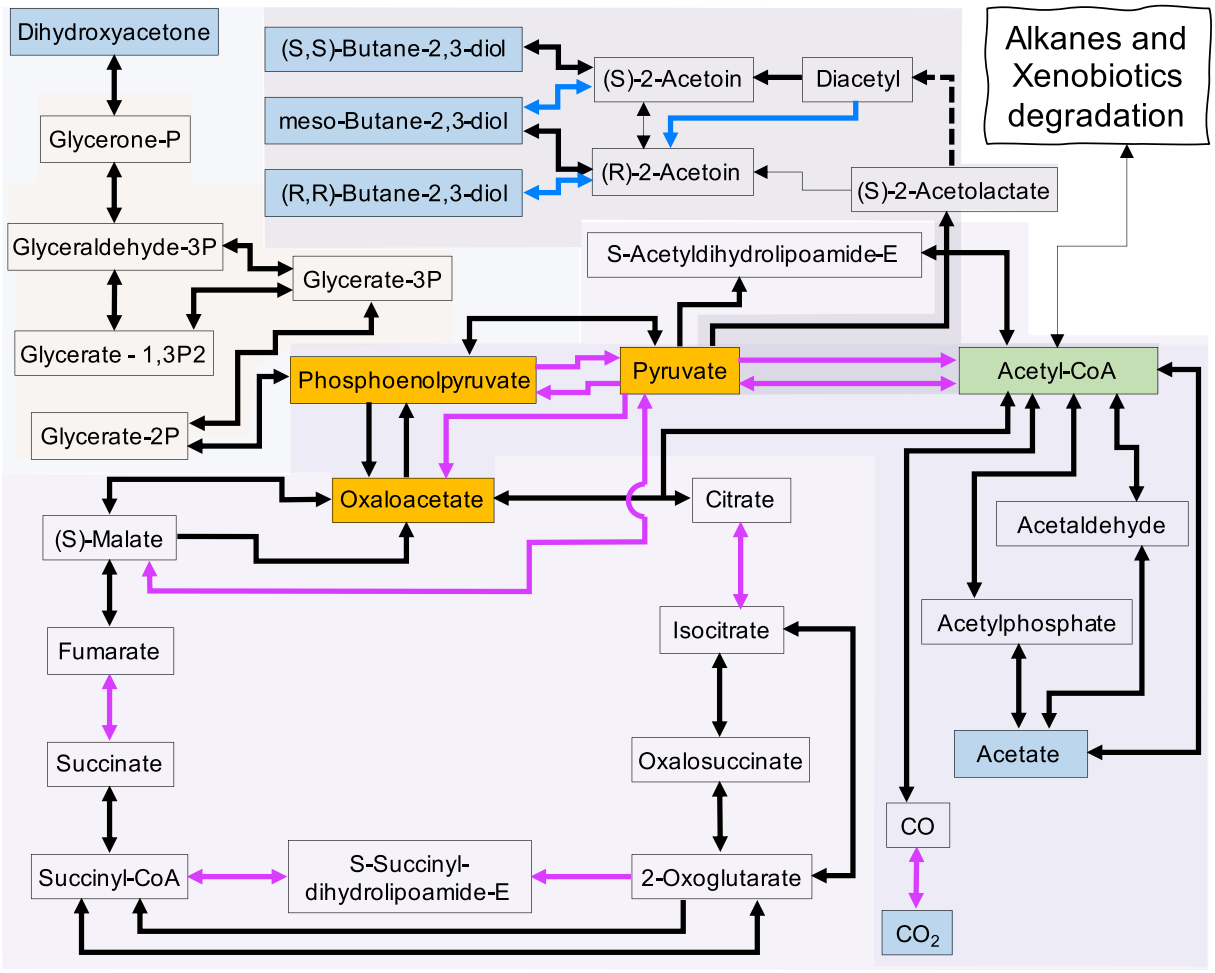


**Fig. 5.** Expression of genes in selected pathways of the Carbohydrate Metabolism and other pathways related to them (i.e., gluconeogenesis, and pyruvate, butanoate and methane metabolism; KEGG database, https://www.genome.jp/kegg/) at the end of 7 weeks of incubation in sediments contaminated with Statfjord oil, in HPS and APS. Molecules which are enzymatically converted between one another are connected by arrows (multiple arrows between the same two boxes indicate different enzymes, see also KEGG database). Thin arrows indicate that the enzyme exists, but was not expressed in either HPS or APS. Dotted lines indicate that the reaction is not enzymatic. Bold arrows in either black, blue or purple indicate expression of the enzyme. In particular, blue arrows indicate an upregulation in HPS, while arrows in purple upregulation in APS. Up- or down-regulation refer to statistically different levels of expression. (For interpretation of the references to color in this figure legend, the reader is referred to the Web version of this article.)

*Chloroflexia* were again only present in HPS (8% of all fpkm, $P = 0.018$; Table S5D).

Besides, in HPS there was a higher transcript abundance for the metabolism of alternative sulfur-species to $SO_4^{2-}$ (i.e. trithionate [$S_3O_6^{2-}$], thiosulfate [$S_2O_3^{2-}$] and, potentially, alkanesulfonate) to generate $SO_3^{2-}$, which is eventually reduced to $H_2S$ (Fig. 4, Table S5D). The alkanesulfonate transport system from the extracellular environment is constituted by K15553, K15554 and K15555. Transcript abundance of K15555 was higher in HPS (all sequences related to *Actinobacteria*), and K15553 sequences from *Clostridia* were only detected in HPS (Fig. 4, Table S5D). However, the transcripts related to alkanesulfonate further conversion to $SO_3^{2-}$ (K04091, K00299) were not detected (Table S5D). $S_3O_6^{2-}$ is converted to $SO_3^{2-}$ by the dissimilatory $SO_3^{2-}$ reductase (K11180 and K11181), with K11181 more abundant in HPS, and significantly more by *Gammaproteobacteria* (Fig. 4, Table S5D). Similarly, transcripts levels for the conversion of $S_2O_3^{2-}$ to $H_2S$ (K08352, K08353 and K08354) were higher in HPS, namely, with K08354 (mainly due to the predominance of *Deltaproteobacteria*, 78% of all fpkm in HPS, $P = 0.047$; Table S5D). *Deltaproteobacteria* transcripts were also significantly more abundant and predominating the subunit K08352 (73% of all fpkm, $P = 0.031$; Fig. 4, Table S5D).

Given the lower $H_2S$ levels in HPS wrt HPC (Fig. S3A-D), the higher transcript abundance for the uptake and conversion of alternative sulfur species than $SO_4^{2-}$ in HPS points to snorkels as electron sinks for a pool of diverse sulfur compounds at increased HP, which are then regenerated to $SO_4^{2-}$ (Fig. S3E,F). In line with these results, there was a different transcript abundance for polysulfide in HPC wrt HPS (Fig. 4). Polysulfide is generated abiotically by the reaction of $H_2S$ and sulfur, with the former highly accumulated in HPC (Fig. S3A-D). Sulfhydrogenase is a heterotetrameric complex formed by K17993, K17994, K17995 and K17996, and it catalyzes the (reversible) elongation of polysulfide using $H_2S$ as substrate and producing molecular hydrogen ($H_2$) as subproduct. In particular, K17993 was more abundant in HPC wrt HPS (Fig. 4, Table S5D), predominantly due to *Dehalococcoidia* and *Gammaproteobacteria* (>60% and >20% of all fpkm, $P = 0.047$ and 0.011, respectively; Fig. 4, Table S5D). Besides, K17995 transcripts from *Clostridia* were significantly higher in HPC (>40% of all fpkm, $P = 0.0001$; Fig. 4, Table S5D).

### 3.4. The impact of increased HP on gene expression

#### 3.4.1. With conductive graphite snorkels (HPS vs. APS)

*3.4.1.1. Carbohydrate metabolism.* While the overall gene expression in

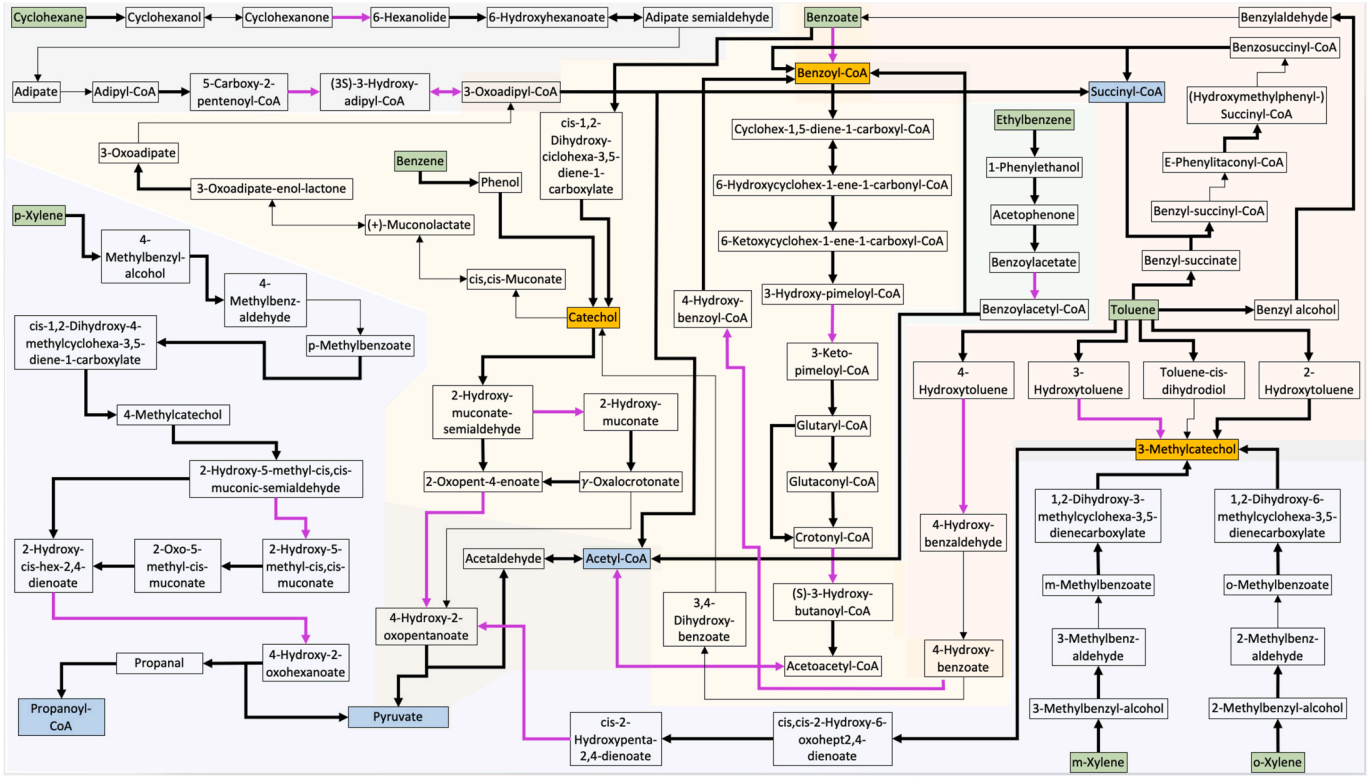


**Fig. 6.** Expression of genes in Xenobiotics metabolism (namely, benzoate, toluene, xylene, caprolactam [ciclohexane] and ethylbenzene; KEGG database, https://www.genome.jp/kegg/) at the end of 7 weeks of incubation in sediments contaminated with Statfjord oil, in HPS and APS. Molecules which are enzymatically converted between one another are connected by arrows (multiple arrows between the same two boxes indicate different enzymes, see also KEGG database). Thin arrows indicate that the enzyme exists, but was not expressed in either HPS or APS. Bold arrows in either black, blue or purple indicate expression of the enzyme. In particular, blue arrows indicate an upregulation in HPS, while arrows in purple upregulation in APS. Up- or down-regulation refer to statistically different levels of expression. (For interpretation of the references to color in this figure legend, the reader is referred to the Web version of this article.)

the TCA cycle pathway (ko00020 in KEGG) was comparable ($P = 0.32$, Fig. S4; Table S7), several specific transcripts were more abundant in APS wrt HPS (Fig. 5, Table S7), indicative of a negative effect of HP increase. Several transcripts were more abundant within the cycle itself in APS, however, the most interesting appear to be the transcripts for the conversion of acetyl-CoA to pyruvate (using reduced ferredoxin; K00169, K00170, and K00172) and its subsequent conversion to oxaloacetate (using ATP, K01960), all more abundant in APS ($P \leq 0.044$, $0.18 < \log2_{fc} < 0.43$; Fig. 5, Table S7). This suggests that in APS oxaloacetate regeneration at the end of the TCA cycle was supported, likely to supply enough co-substrate to acetyl-CoA to initiate the cycle and form citrate. In agreement, transcript levels for the alternative conversion of pyruvate to malate (the precursor of oxaloacetate in the TCA cycle; K00027 and K00029) were also higher in APS ($P = 0.025$, $\log2_{fc} = 0.34$, fpkm = 135 vs. 107; and $P = 0.013$, $\log2_{fc} = 0.32$, fpkm = 123 vs. 99, respectively; Table S7). In agreement with sustained TCA cycle rates in APS, in HPS transcript levels for alternative pathways to process acetyl-CoA were higher, e.g. diacetyl and acetoin conversion to 2,3 butanediol (K00004; $P = 0.012$, $\log2_{fc} = 0.91$, fpkm = 10 *vs.* 5, Fig. 5), with diacetyl deriving from the non-enzymatic conversion of acetolactate, which is connected to acetyl-CoA via pyruvate (all genes annotated, Fig. 5, Table S7).

*3.4.1.2. Xenobiotics biodegradation and metabolism.* The higher removal of TPH in APS wrt HPS ($C/C_0$ equal to 0.64 ± 0.04 vs. 0.87 ± 0.08; Fig. S2B) was generally confirmed by an enhanced transcript level in APS e.g. for benzoate, caprolactam, nitrotoluene and toluene degradation pathways ($P < 0.05$, Fig. 1). For instance (Fig. 6), the conversion of benzoate into acetyl-CoA (entering the TCA cycle) involves 26 genes, of which only one could not be annotated (E.C.:1.1.1.259; however, K01782, K01825 and K07516 performing the same reaction were annotated; Table S7). Of these 25 annotated genes, six genes involved in four conversion steps had higher transcript levels in APS (K04140, K04105, K01782, K01825, K01692 and K00626; $P \leq 0.037$, $0.45 < \log2_{fc} < 1.34$; Fig. 6, Table S7). In particular, K04140 and K04105 were exclusively detected in APS, and entirely due to *Clostridia* ($P = 0.001$, fpkm = 6 vs. 0 for each gene; Table S8E). This also concerned the conversion of benzene to acetyl-CoA, via the initial conversion to phenol and then catechol: of the 19 annotated genes only a (non-essential) gene could not be annotated (E.C.:4.1.1.-), while the transcripts for three genes covering two conversion steps were more abundant in APS (K10217, K02554 and K18364; $P \leq 0.038$, $2.02 < \log2_{fc} < 4.08$; Fig. 6, Table S7). *Gammaproteobacteria* constituted 100% of all the sequences in APS for each of these three genes (Table S8E). The benzoate degradation pathway apparently also acted as a recipient of other metabolic routes at either HP, although higher transcript levels were only found in APS. For instance, 8/12 genes involved in the degradation of ethylbenzene into benzoyl-CoA and acetyl-CoA were annotated, with one transcript more abundant in APS over five conversion steps (K14747; $P = 0.038$, $\log2_{fc} = 1.40$, fpkm = 13 vs. 5; Fig. 6, Table S7). Similarly, 7/9 genes involved in the conversion of toluene to benzoyl-CoA entering the benzoate degradation pathway were annotated (Fig. 6, Table S7), with two more abundant in APS over six conversion steps (K05797; $P = 0.018$, $\log2_{fc} = 2.97$, fpkm = 7 vs. 1; and K04105; $P = 0.001$, fpkm = 6 vs. 0; Fig. 6, Table S7). However, toluene can also be converted to 3-methylcatechol and enter the xylene degradation pathway (9/18 genes annotated; of which K03380 more abundant in APS; $P = 0.035$, $\log2_{fc} = 1.65$, fpkm = 4 vs. 1; Fig. 6, Table S7).

In the xylene degradation pathway, almost all the many genes involved in the degradation of either *p*-, *o*-, or *m*-xylene were detected

(Fig. 6, Table S7). In particular, generation of 3-methylcatechol from toluene can continue with conversion of the former into acetyl-CoA to enter the TCA cycle (7/10 genes were annotated, with K02554 and K18364 involved in the same reaction which had higher transcript levels in APS, respectively: $P = 0.038$, $\log2_{fc} = 2.02$, fpkm = 5 vs. 1; and $P = 0.002$, $\log2_{fc} = 4.08$, fpkm = 5.5 vs. 0.3; Fig. 6, Table S7). Finally, in the caprolactam degradation pathway, the route specifically converting cyclohexane to eventually oxadipyl-CoA had also higher transcript levels in APS: 12/23 genes in this metabolic route were annotated, of which four with more abundant transcripts in APS (in three conversion steps, namely, K01692, K01782, K01825 and K03379; $P \leq 0.037$, $0.59 < \log2_{fc} < 2.55$; Fig. 6, Table S7). In particular, *Gammaproteobacteria* were the predominant taxa in all of these four genes (up to 100% of all sequences), being significantly more abundant in APS in 3/4 cases ($P \leq 0.017$; Table S8I). Oxadipyl-CoA can then be converted to succinyl-CoA (via the annotated K00632) to enter the TCA cycle or to act as intermediate in the toluene degradation pathway (Fig. 6).

*3.4.1.3. Energy metabolism: sulfur.* In both HPS and APS, transcript levels in the energy-generating dissimilatory $SO_4^{2-}$ reduction was higher wrt assimilatory ($P \leq 0.009$, $\log2_{fc} \geq 1.65$; Table S9A,B). However, transcript levels for the energy-consuming assimilatory $SO_4^{2-}$ reduction were lower in HPS wrt APS ($P = 0.016$, $\log2_{fc} = 0.52$, fpkm = 587 vs. 411; Table S9B). In the context of a higher crude oil biodegradation (Fig. S2B,D) and enhanced expression of several key genes in the TCA cycle in APS wrt HPS (Fig. 5), this suggests that in the presence of snorkels, the increase in HP (HPS vs. APS) affected the energy management by the cells, despite in HPS an active degradation of alkanes took place (Fig. S2D). In particular, in the assimilatory pathways transcript levels for the conversion of $SO_4^{2-}$ to adenylyl $SO_4^{2-}$ and PAPS were higher in APS (K13811; $P = 0.019$, $\log2_{fc} = 1.47$, fpkm = 27 vs. 10; and K00860; $P = 0.035$, $\log2_{fc} = 1.26$, fpkm = 23 vs. 10; Table S7). Transcript levels for the final reduction of $SO_3^{2-}$ into $H_2S$ in the assimilatory pathway was also higher in APS ($\log2_{fc} = 0.61$, fpkm = 218 vs. 143), albeit less significantly ($P = 0.051$; Table S7) (it was almost uniquely due to *Gammaproteobacteria*, >99% of all fpkm in either APS or HPS; Table S8D; overview in Fig. S24).

### 3.4.2. With non-conductive glass controls (HPC vs. APC)

*3.4.2.1. Carbohydrate metabolism.* Transcript levels in the TCA cycle were comparable in HPC and APC (Fig. S25). This was in sharp contrast with the negative effect of increased HP in the presence of snorkels (Fig. 5), and suggests that snorkels application can in fact stimulate microbial metabolism, particularly at ambient pressure. Nonetheless, slightly higher transcript levels for alternative pathways to metabolize acetyl-CoA were noted when increasing HP in HPC wrt APC (Fig. S25; Table S10,S11A-K). This effect on metabolism as induced by a HP increase was also noted with snorkels (HPS vs. APS; Fig. 5), but it also resulted from snorkels application at ambient pressure (APS vs. APC; Fig. 2A). One alternative pathway with higher transcript levels in HPC wrt APC was the acetyl-CoA pathway, leading to the oxidation of acetyl-CoA to CO (K00194; $P = 0.025$, $\log2_{fc} = 0.38$, fpkm = 168 vs. 129, HPC vs. APC) and then to $CO_2$ (K00195; $P = 0.044$, $\log2_{fc} = 0.32$, fpkm = 23 vs. 18, HPC vs. APC; Table S10). Another pathway with higher transcript levels was that transforming acetyl-CoA to acetaldehyde (K04021; $P = 0.036$, $\log2_{fc} = 0.34$, fpkm = 7 vs. 6; Table S10) and then to acetate (K00128; $P = 0.007$, $\log2_{fc} = 0.27$, fpkm = 61 vs. 51; Table S10). An additional pathway with slightly higher transcript levels converted acetyl-CoA to acetoacetyl-CoA (K00626; $P = 0.012$, $\log2_{fc} = 0.16$, fpkm = 461 vs. 413; Table S10), particularly due to *Deltaproteobacteria* (>30% of all fpkm, $P = 0.017$; Table S11J). Transcript levels for acetoacetyl-CoA conversion to (S)-3-Hydroxy-3-methylglutaryl-CoA via fusion via another acetyl-CoA were also slightly higher (K01641; $P = 0.024$, $\log2_{fc} = 0.13$, fpkm = 85 vs. 78; Table S10). (S)-3-Hydroxy-3-methylglutaryl-CoA can then enter the mevalonate pathway for the biosynthesis of terpenoids backbone. Finally, acetyl-CoA may have also fed the pathway leading to dihydroxyacetone: all the 16 genes involved in this pathway were detected, and the transcript levels of two were more abundant in HPC wrt APC, particularly the last reaction. These include K01689 ($P = 0.030$, $\log2_{fc} = 0.17$, fpkm = 170 vs. 151, Table S10) and K00863 ($P = 0.036$, $\log2_{fc} = 0.75$, fpkm = 59 vs. 35; Table S10). For either sequence, higher transcript levels in HPC were generally due to *Clostridia* (20–40% of all fpkm in both K01689and K00863; Table S11K).

### 3.5. Microbial community assemblage in sediments, and biofilms on snorkels surface

Alkane-rich (15%), Statfjord-oil-contaminated sediments were analyzed for their microbial community assemblage using 16S rRNA gene amplicon sequencing. The predominant bacterial taxa were *Chloroflexi*, *Epsilonbacteraeota, Deltaproteobacteria*, *Firmicutes* and *Gammaproteobacteria* (each in general >5% and, altogether, >80% in any treatment; Table S12A). This is in agreement with meta-transcriptomic data indicating *Deltaproteobacteria*, *Gammaproteobacteria* and *Clostridia (Firmicutes)* as predominant taxa (~33, 23 and 19%, respectively, across all samples; Table S13). All taxa remained constant in each treatment wrt their initial concentration ($T_0$; Table S12A,B), with the exception of *Firmicutes* whose relative abundance increased at the end of the experiment ($\log2_{fc} \geq 1.77$ in either treatment; Table S12A). The deepest taxa forming a core community of recurrently present microorganisms (generally >5%) amounted to 40–50% in all treatments, and included the *Dehalococcoidia* SCGC-AB-539-J10, an uncultured *Anaerolineaceae (Anaerolineae)*, *Fusibacter (Clostridia)*, and *Sulfurimonas* and *Sulfurovum* (*Epsilonproteobacteria*) (Table S12B). In particular, the relative abundance of *Sulfurimonas* increased in contaminated sediments with snorkels wrt glass controls, irrespective of the HP applied ($\log2_{fc} = 1.10$; Table S12B).

Among the less abundant satellite microbial taxa (generally <3%) the contamination with Statfjord oil enriched an unclassified *Clostridiales* JTB215 ($\log2_{fc} \geq 2.99$; Table S12B). The latter was generally enriched in glass controls wrt snorkels, and suppressed with increased HP ($\log2_{fc} \leq -0.55$; Table S12B). Oil contamination was consistent with a rearrangement of *Deltaproteobacteria* satellite species irrespective of HP or snorkels application: the enrichment of *Desulfuromonas* ($\log2_{fc} \geq 1.18$), *Desulfuromusa* ($\log2_{fc} \geq 1.71$) and *Desulfocapsa* ($\log2_{fc} \geq 0.96$ with the exception of APC; Table S12B) occurred in contrast to the reduction of *Desulfatiglans* ($\log2_{fc} \leq -0.33$; Table S12B). In particular, *Desulfuromusa* was slightly higher in sediments with snorkels ($\log2_{fc} \geq 0.23$; Table S12B). To confirm the impact of snorkels on microbial community assemblage in a comparable setup, the 16 S rRNA gene analysis was also conducted with the alkane-poor (4%), DUC-oil-contaminated sediments, and the same exact trends were noted (Table S12C,D; a deeper analysis in Supplementary Information).

Microbial community assemblage was also analyzed on the biofilm of snorkels (Table 1, complete dataset in Table S13A-C). Since the assemblage in sediments was essentially equal with either crude oil (alkane rich or poor, 15 vs. 4%), these two data sets were analyzed together to better assess which taxa was recurrently more abundant on snorkels biofilms wrt the surrounding sediment. Three groups could be identified (Table 1; Table S13A-C): i) taxa enriched on snorkels biofilms at either HP (Table S13A-C), with the most relevant (enriched to ≥0.5%, $\log2_{fc} \geq 0.20$) being *Draconibacterium* and *Desulfuromusa*; ii) taxa enriched on snorkels biofilms only at increased HP (Table S13B), with the most relevant an unclassified *Oxyphotobacteria* (Cyanobacteria), *Sulfitobacter* and *Thiomicrorhabdus*; and iii) taxa enriched on biofilms only at ambient pressure (Table S13C), with the most relevant an unclassified Bradymonadales (*Deltaproteobacteria*), *Desulfoconvexum*, *Thioalkalispira*, an unclassified Bacteria and *Sulfurimonas*. Notably, *Sulfurimonas* was the only OTU belonging to the core community in sediments (Table S12B,D) to be also enriched on snorkels, while the

**Table 1**
Relative abundance of 16S rDNA sequences, and log2 fold change in microbial communities collected from either the surface of graphite snorkels or from the sediment (see Table S10) after 7 weeks of incubation with either Statfrjod or DUC crude oil, at either increased or ambient hydrostatic pressure (10 or 0.1 MPa, respectively). Heatmaps represent high (green) or low (red) relative abundance, and high increase (blue) or high decrease (red) in log2 fold change in the tested condition.

| | | | | SNORKEL | | | | SEDIMENT | | | | SNORKEL *vs*. SEDIMENT | | | |
|---|---|---|---|---|---|---|---|---|---|---|---|---|---|---|---|
| | | | | Relative abundance % | | | | Relative abundance % | | | | Log2 fold change | | | |
| | | | Crude oil | Statfjord | | DUC | | Statfjord | | DUC | | Statfjord | | DUC | |
| Phylum | Class | Deepest taxon | Hydrostatic Pressure (MPa) | 10 | 0.1 | 10 | 0.1 | 10 | 0.1 | 10 | 0.1 | 10 | 0.1 | 10 | 0.1 |
| Actinobacteria | Actinobacteria | Cutibacterium | | 0.2 | 0.0 | 2.3 | 6.0 | 0.0 | 0.0 | 0.0 | 0.0 | - | - | - | - |
| Proteobacteria | Alphaproteobacteria | Picochlorum sp. SENEW3 | | 0.2 | 0.0 | 1.1 | 0.0 | 0.0 | 0.0 | 0.0 | 0.0 | - | - | - | - |
| Proteobacteria | Gammaproteobacteria | Colwellia | | 0.0 | 0.0 | 0.1 | 1.7 | 0.0 | 0.0 | 0.0 | 0.0 | - | - | - | - |
| Proteobacteria | Deltaproteobacteria | unclassified Bradymonadales | | 0.8 | 1.4 | 0.0 | 2.6 | 0.0 | 0.0 | 0.0 | 0.0 | - | - | - | - |
| Bacteroidetes | Bacteroidia | unclassified Bacteroidetes VC2.1 Bac22 | | 0.1 | 0.1 | 0.0 | 1.0 | 0.0 | 0.1 | 0.0 | 0.0 | - | 0.07 | - | - |
| Proteobacteria | Gammaproteobacteria | Aestuariicella | | 0.0 | 0.0 | 0.0 | 7.9 | 0.0 | 0.0 | 0.0 | 0.1 | - | - | - | 6.50 |
| Epsilonbacteraeota | Campylobacteria | Arcobacter | | 0.0 | 0.2 | 3.8 | 1.9 | 0.2 | 0.5 | 0.5 | 0.2 | - | -1.28 | 2.92 | 2.97 |
| Proteobacteria | Gammaproteobacteria | Pseudomonas | | 0.2 | 0.1 | 0.1 | 1.6 | 0.0 | 0.0 | 0.0 | 0.9 | - | - | 1.25 | 0.81 |
| Proteobacteria | Deltaproteobacteria | Desulfuromonas | | 8.2 | 5.4 | 3.0 | 2.7 | 0.8 | 1.1 | 3.7 | 2.6 | 3.38 | 2.35 | -0.30 | 0.05 |
| Proteobacteria | Deltaproteobacteria | unclassified Desulfuromonadales | | 0.8 | 1.5 | 0.0 | 0.2 | 0.1 | 0.3 | 0.0 | 0.0 | 3.02 | 2.29 | - | - |
| Chloroflexi | Dehalococcoidia | uncultured S085 | | 2.3 | 0.6 | 0.1 | 0.0 | 0.3 | 0.2 | 0.4 | 0.3 | 2.85 | 1.82 | -1.88 | - |
| Bacteroidetes | Bacteroidia | Draconibacterium | | 1.7 | 5.1 | 0.8 | 1.2 | 0.3 | 0.1 | 0.2 | 0.3 | 2.65 | 5.10 | 1.97 | 2.00 |
| Actinobacteria | Thermoleophilia | uncultured 67-14 | | 0.2 | 0.0 | 2.9 | 0.5 | 0.0 | 0.0 | 0.0 | 0.0 | 2.61 | - | 6.11 | - |
| Proteobacteria | Deltaproteobacteria | Desulfuromusa | | 7.4 | 5.8 | 2.4 | 4.8 | 1.3 | 1.5 | 1.1 | 1.4 | 2.53 | 1.96 | 1.11 | 1.82 |
| Cyanobacteria | Oxyphotobacteria | unclassified Oxyphotobacteria | | 1.3 | 0.1 | 11.6 | 6.1 | 0.3 | 0.5 | 0.5 | 0.5 | 2.35 | -2.32 | 4.65 | 3.65 |
| Proteobacteria | Alphaproteobacteria | Sulfitobacter | | 1.4 | 0.6 | 2.0 | 10.1 | 0.5 | 0.6 | 1.2 | 8.8 | 1.56 | -0.08 | 0.71 | 0.20 |
| Firmicutes | Clostridia | unclassified Clostridiales | | 1.4 | 1.5 | 0.8 | 0.3 | 0.7 | 0.6 | 0.9 | 2.1 | 1.06 | 1.26 | -0.24 | -2.84 |
| Proteobacteria | Deltaproteobacteria | Desulfocapsa | | 3.3 | 1.3 | 1.0 | 0.3 | 1.7 | 1.8 | 1.2 | 0.7 | 0.95 | -0.48 | -0.21 | -1.28 |
| Proteobacteria | Gammaproteobacteria | Thiomicrorhabdus | | 4.4 | 4.3 | 5.3 | 1.9 | 2.7 | 3.2 | 3.0 | 4.0 | 0.73 | 0.42 | 0.83 | -1.08 |
| Proteobacteria | Deltaproteobacteria | Desulfoconvexum | | 0.5 | 3.2 | 0.3 | 2.2 | 0.4 | 1.2 | 0.4 | 0.7 | 0.44 | 1.47 | -0.45 | 1.68 |
| Chloroflexi | Anaerolineae | uncultured Anaerolineaceae | | 9.6 | 5.4 | 3.8 | 3.2 | 7.4 | 6.7 | 7.1 | 8.7 | 0.38 | -0.30 | -0.90 | -1.44 |
| Proteobacteria | Deltaproteobacteria | uncultured Sva1033 | | 0.2 | 1.3 | 0.1 | 0.2 | 0.2 | 0.4 | 0.3 | 1.3 | 0.22 | 1.81 | -1.75 | -2.67 |
| Proteobacteria | Alphaproteobacteria | Methyloceanibacter | | 0.4 | 0.0 | 3.4 | 0.1 | 0.4 | 0.4 | 0.5 | 0.2 | 0.18 | - | 2.87 | -1.16 |
| Epsilonbacteraeota | Campylobacteria | Sulfurovum | | 8.6 | 2.9 | 1.2 | 2.2 | 7.7 | 7.9 | 6.8 | 8.7 | 0.16 | -1.45 | -2.51 | -1.98 |
| Proteobacteria | Gammaproteobacteria | Thioalkalispira | | 0.2 | 3.0 | 0.2 | 0.7 | 0.2 | 1.8 | 0.2 | 0.0 | 0.08 | 0.74 | 0.04 | - |
| Proteobacteria | Alphaproteobacteria | unclassified Rhodobacteraceae | | 3.9 | 1.4 | 1.4 | 1.6 | 3.8 | 2.1 | 1.3 | 2.1 | 0.03 | -0.55 | 0.14 | -0.38 |
| unknown | | unclassified Bacteria | | 2.5 | 2.5 | 4.5 | 4.4 | 2.6 | 2.1 | 3.0 | 1.9 | -0.05 | 0.23 | 0.61 | 1.18 |
| Chloroflexi | Dehalococcoidia | uncultured MSBL5 | | 2.4 | 3.7 | 0.8 | 0.0 | 2.9 | 3.4 | 3.4 | 4.0 | -0.25 | 0.10 | -2.09 | - |
| Proteobacteria | Gammaproteobacteria | unclassified Gammaproteobacteria | | 0.6 | 0.1 | 0.9 | 0.2 | 0.8 | 0.4 | 0.3 | 0.2 | -0.42 | -2.01 | 1.42 | 0.12 |
| Chloroflexi | Dehalococcoidia | uncultured AB-539-J10 | | 0.6 | 1.1 | 0.2 | 0.1 | 0.8 | 1.1 | 0.5 | 0.5 | -0.47 | -0.02 | -1.30 | -2.19 |
| Firmicutes | Clostridia | Fusibacter | | 5.1 | 3.1 | 1.1 | 1.1 | 8.1 | 5.2 | 15.7 | 13.6 | -0.66 | -0.75 | -3.84 | -3.63 |
| Epsilonbacteraeota | Campylobacteria | Sulfurimonas | | 3.4 | 12.1 | 4.5 | 5.2 | 7.8 | 10.1 | 4.7 | 3.3 | -1.19 | 0.27 | -0.06 | 0.67 |
| Bacteroidetes | Bacteroidia | unclassified Bacteroidia | | 0.1 | 0.3 | 0.4 | 1.0 | 0.2 | 0.0 | 0.1 | 0.1 | -1.25 | - | 1.79 | 3.52 |
| Bacteroidetes | Bacteroidia | unclassified Bacteroidetes BD2-2 | | 0.3 | 0.2 | 0.2 | 0.2 | 1.2 | 1.6 | 1.0 | 0.3 | -2.01 | -2.96 | -2.25 | -0.59 |
| Chloroflexi | Dehalococcoidia | SCGC-AB-539-J10 | | 9.0 | 12.9 | 1.0 | 0.7 | 36.8 | 38.4 | 30.1 | 25.5 | -2.03 | -1.57 | -4.91 | -5.19 |
| | | | Relative total abundance | 81.3 | 81.2 | 61.3 | 73.9 | 89.8 | 93.2 | 88.1 | 93.0 | | | | |

relative abundance of the other four OTUs in the sediment core community were typically lower on biofilms (Table 1). This clearly indicates that OTU abundance on snorkels biofilms was unrelated to OTU abundance in sediments.

### 3.6. AVS and $Fe^{2+}$ levels in sediments

The dynamics of FeS (AVS) was correlated to that of reduced $SO_4^{2-}$ and accumulated $H_2S$. High $SO_4^{2-}$ depletion in the pore water of Statfjord-oil-contaminated sediments (Fig. S3F) was consistent with increasing AVS levels wrt $T_0$ (Fig. S26A). Besides, the high levels of $H_2S$ oxidation when using snorkels wrt glass controls (Fig. S3C,D) were reflected into lower AVS levels, at either HP (Fig. S26A). The pH minima in sediments were consistent with these trends (Fig. S27): with snorkels, sediments had lower pH values wrt glass controls, overall suggestive of mild acidification owing to snorkels anodic reactions.

$Fe^{2+}$ levels were generally higher at 10 wrt 0.1 MPa (Fig. S26B). Such HP impact was remarkable and no correlation with AVS was noted. $Fe^{2+}$ was thus analyzed also on poor-alkane (4%), DUC-oil-contaminated sediments, where a similar trend was observed (Fig. S28).

### 3.7. Elemental composition of the snorkels surface

At the end of the incubation with crude oil, Aluminum (Al, 2.4 atomic %), Fe (1.2 atomic %) and phosphorous (P, 2.1 atomic %) were found in snorkels exposed to increased HP but not at ambient pressure (Table 2). This was confirmed when analyzing snorkels applied to DUC-oil-contaminated sediments (0.8, 1.2 and 2.1 atomic %, respectively; Table 2). Fe was composed of both $Fe^{2+}$ and $Fe^{3+}$ species (with Statfjord oil) or only $Fe^{3+}$ (with DUC oil). Silicon (Si) in the form of silicate ($SiO_2$) was detected on the surface of all tested snorkels, however, its relative abundance was apparently higher at increased HP (3.8 vs. 2.1 atomic % with Statfjord oil; confirmed with DUC oil, 2.9 vs. 2.2 atomic %; Table 2). No elemental sulfur ($S^0$) was detected on the surface of snorkels. However, when using DUC oil about 1 atomic % was detected (owing to C–S compounds or $SO_4^{2-}$; Table 2).

## 4. Discussion

Bioremediation of marine environments exposed to mild HPs (e.g. 10 MPa) is limited by the negative HP effects imposed on the predominant piezosensitive heterotrophs. Such limitations are further stressed in anaerobic sediments. Graphite rods (snorkels) bridging anaerobic sediments to aerobic overlaying waters allow microbial cells in sediments to breath oxygen while physically residing close to the energy-rich electron donors (e.g. hydrocarbons). Snorkels can thus act as virtually inexhaustible electron acceptors either directly or via shuttle molecules (e.g. reduced sulfur species). Application of snorkels to remote, oil-contaminated deep-sea sediments is unlikely. However, snorkels are extremely handy tools to test in the laboratory if and how electrochemistry can enhance oil biodegradation at deep-sea conditions. In (Aulenta et al., 2021), we reported that snorkels can enhance alkanes oxidation at 10 MPa. Here, we show that this depends on the fact that both snorkels and increased HP impact the oxidation of acetyl-CoA in

**Table 2**
X-ray photoelectron spectroscopy (XPS) analysis of the elements present on the surface of the graphite snorkels after 7 weeks of incubation with either Statfjord or DUC crude oil, at either increased or ambient hydrostatic pressure (AP or HP, 10 or 0.1 MPa, respectively). Negative controls at time zero reports on XPS analysis prior to any biological process, that is, a standard snorkel as provided by the manufacturer.

| Negative control | | | STATFJORD oil | | | | | | DUC oil | | | | | |
|---|---|---|---|---|---|---|---|---|---|---|---|---|---|---|
| Time zero | | | HPS | | | APS | | | HPS | | | APS | | |
| Peak | Atomic % | State | Peak | Atomic % | State | Peak | Atomic % | State | Peak | Atomic % | State | Peak | Atomic % | State |
| | | | Al | 2.4 | $Al_2O_3$ | | | | Al | 0.8 | $Al_2O_3$ | | | |
| C | 95.9 | C–C | C | 45.9 | C–C | C | 70.9 | C–C | C | 59.3 | C–C | C | 66.6 | C–C |
| | | | C | 12.0 | C–O | C | 12.9 | C–O | | | | | | |
| | | | C | 5.2 | C═O | C | 3.9 | C═O | | | | | | |
| | | | C | 1.3 | carboxyl | | | | | | | | | |
| | | | Ca | 1.5 | | Ca | 0.7 | | Ca | 0.8 | | | | |
| | | | | | | Cl | 0.3 | Cl- | Cl | 2.1 | | Cl | 7.7 | |
| | | | Fe | 0.5 | Fe(II) | | | | Fe | 1.2 | Fe(III) | | | |
| | | | Fe | 0.7 | Fe(III) | | | | | | | | | |
| | | | Mg | 0.6 | | | | | Mg | 1.1 | | Mg | 2.9 | |
| | | | | | | | | | N | 2.4 | | N | 1.4 | |
| | | | | | | | | | Na | 1.3 | | Na | 2.9 | |
| O | 2.0 | C–O, OH- | O | 17.7 | C–O, OH- | O | 9.2 | $H_2O$, C═O | O | 24.8 | | O | 15.4 | |
| | | | O | 5.7 | $H_2O$, C═O | | | | | | | | | |
| O | 0.9 | $SiO_2$ | | | | | | | | | | | | |
| | | | P | 2.1 | | | | | P | 2.1 | | | | |
| | | | | | | | | | S | 0.8 | C–S | S | 0.2 | C–S |
| | | | | | | | | | S | 0.4 | sulphates | S | 0.7 | sulphates |
| | | | Si | 0.6 | SiC | Si | 2.1 | $SiO_2$ | Si | 2.9 | | Si | 2.2 | SiO2 |
| Si | 0.9 | $SiO_2$ | Si | 3.2 | $SiO_2$ | | | | | | | | | |
| | | | Si | 0.6 | $SiO_2$ | | | | | | | | | |
| Cl | 0.3 | chloride | | | | | | | | | | | | |
| **Total** | **100.0** | | **Total** | **100.0** | | **Total** | **100.0** | | **Total** | **100.0** | | **Total** | **100.0** | |

the TCA cycle.

### 4.1. Increased HP challenges the TCA cycle rather than beta oxidation also in anaerobic sediments

Increased HP challenges cell homeostasis and slows down microbial metabolism (Bartlett, 2002; Bartlett et al., 1995). Transcriptomics and metaproteomics studies with aerobic, pure (Scoma et al., 2016a, 2016b), mixed or synthetic cultures (Scoma et al., 2018) repeatedly indicated that the main pathway for hydrocarbons oxidation (i.e. *beta* oxidation) is not impacted by increased HP. This is confirmed in the present meta-transcriptomic dataset in anaerobic sediments (Fig. S9-22). Reduced oil degradation at increased HP in piezosensitive microorganisms thus depends on other metabolic pathways, e.g. the following TCA cycle.

The TCA cycle is negatively affected by a HP increase. Hydrocarbon-degrading synthetic communities (originally collected at 1000 m bswl) accumulated citrate and dihydroxyacetone intracellularly when exposed aerobically to *in situ* pressures of 10 MPa (Scoma et al., 2018). This indicated that the TCA cycle was slowed down and that the excess carbon available by the cell was diverted to carbon reserves (dihydroxyacetone) (Scoma et al., 2018). This response was also observed in controls only supplied with acetate (Scoma et al., 2018).

The main aim of the TCA cycle is to fully oxidize acetyl-CoA to generate reduced electron carriers (NADH and $FADH_2$) (Berg et al., 2015). The TCA cycle itself does not require oxygen, and the several metabolic intermediates can leave the cycle and become the substrate of primary anabolic pathways (e.g. amino acid and carbohydrate metabolism). However, under aerobic conditions NADH and $FADH_2$ can eventually use oxygen as ultimate electron acceptor in the subsequent oxidative phosphorylation to generate ATP (Berg et al., 2015). As *beta* oxidation is not impacted by increased HP and cells accumulate dihydroxyacetone despite being tested aerobically (Scoma et al., 2018), ATP synthesis may not represent the main (or sole) process limiting cell metabolism (Scoma et al., 2016a, 2016b) (Scoma et al., 2018). It can rather be inferred that increased HP challenges the cell's capacity to manage high levels of acetyl-CoA and/or the reducing power resulting from its oxidation in the TCA cycle. This is in agreement with our data showing that snorkels enhanced alkanes oxidation at increased HP under anaerobic conditions (Fig. S2D (Aulenta et al., 2021)). The role of snorkels is to act as major electron acceptors in sediments. The oxidation of e.g. reduced sulfur and iron species (Viggi et al., 2015, 2017) provides new oxidized electron carriers for the reducing power derived from the biological oxidation of organic matter, including crude oil (Viggi et al., 2015, 2017). The metabolism of acetyl-CoA was thus investigated more in depth.

### 4.2. Snorkels application is associated with higher transcript levels in the TCA cycle, or lower transcripts in alternative pathways for acetyl-CoA

The application of conductive snorkels rather than non-conductive glass controls enhanced the transcript levels of TCA cycle genes at ambient pressure (APS vs. APC) (Fig. 2A), suggesting that this cycle remained the primary sink for the high amount of acetyl-CoA derived from hydrocarbons degradation (Fig. S2B,D). In glass controls (APC), acetyl-CoA was apparently diverted to 2,3 butanediol formation (Fig. 2A). The latter pathway is featured by the oxidation of reduced electron carriers (e.g. reduced ferredoxin or NADH; KEGG reaction numbers R01196, R02855, R02946 and R10504, see Supplementary Information). In the frame of comparable transcript levels for alkanes activation and *beta* oxidation (Fig. S9-22) and xenobiotics biodegradation (Fig. 3), this suggests that: 1) microbial communities in anaerobic sediments were able to initially engage in hydrocarbons oxidation comparably well with and without snorkels; 2) the application of snorkels allowed the intracellular reducing power generated from hydrocarbons oxidation (e.g. in the TCA cycle) to be quickly used by the cell; 3) in the absence of snorkels, the high reducing power available by the cells eventually affected the TCA cycle itself, and stimulated alternative pathways which concomitantly used the accumulated reduced electron

carriers and acetyl-CoA. Microbial taxa such as *Clostridia* and *Alphaproteobacteria* appear particularly involved in this alternative pathway (Table S3J).

Results at increased HP confirm this hypothesis (HPS vs. HPC): while snorkels application did not result into higher transcript levels of TCA-related genes, in glass controls (HPC) transcript levels of genes processing acetyl-CoA via alternative routes were higher (Fig. 2B). These generated either reducing power (i.e. reduced ferredoxin, via oxidation to $CO_2$) or ATP (via conversion to acetate; see Supplementary Information). *Deltaproteobacteria* and *Clostridia* mainly engaged in these pathways at increased HP (Table S5K). The fact that reduced electron carriers were generated (rather than dissipated) in HPC wrt HPS may appear contradictory, as these could directly result from acetyl-CoA oxidation in the TCA cycle itself. However, microbial needs at increased HP may differ wrt ambient pressure, e.g. in the case of energy management. It could be speculated that regulation of reducing power by the cells in HPC may have been controlled via intracellular accumulation of dihydroxyacetone, particularly in *Clostridia* which predominated these sequences (Table S5B,K). The reactions connecting acetyl-CoA to dihydroxyacetone generation entail no net ATP consumption; and while consuming acetyl-CoA and reducing power they store a carbon and energy reserve intracellularly (see Supplementary Information for all reaction steps). The intracellular accumulation of dihydroxyacetone in cells with an impaired TCA cycle under similar conditions supports this hypothesis (i.e. hydrocarbon-degrading cells at 10 wrt 0.1 MPa (Scoma et al., 2018);).

Concerning 2,3 butanediol, its exact metabolic role remains uncertain (Ji et al., 2011). It was proposed to prevent intracellular acidification and balance NADH/$NAD^+$ levels (as pyruvate fermentation would shift from acetate or ethanol generation to 2,3 butanediol, which is a neutral metabolite and regenerates $NAD^+$) (Johansen et al., 1975; Magee and Kosaric, 1987; Tsau et al., 1992; Van Houdt et al., 2007). Owing to its reversible reaction to acetoin, 2,3 butanediol is regarded as a carbon and energy reserve for the cell (Xiao and Xu, 2007). 2,3 butanediol also acts as an anti-freezing compound due to its low freezing point (−60 °C (Li et al., 2010);). Low temperature and increased HP may impose similar effects on cells, such as an increased packing of phospholipid fatty acids on the membrane (reviewed in (Capece et al., 2013)), affecting protons influx/efflux thus intracellular pH (Abe and Horikoshi, 1998; Diomande et al., 2015; Enns et al., 1965; Oger and Jebbar, 2010). Cells normally maintain a slightly more alkaline pH wrt to the extracellular environment. Increased membrane damage in piezosensitive bacteria as resulting from a reduced membrane fluidity can thus increase cell acidification, as protons may leak back into the cell (Abe and Horikoshi, 1998; Diomande et al., 2015; Enns et al., 1965; Oger and Jebbar, 2010). Cells at increased HP actively degrading alkanes but with an increasingly impaired TCA cycle may thus find advantageous to slightly accumulate 2,3 butanediol as a potential piezolyte and carbon reserve, which also regulates NADH/$NAD^+$ levels and counterbalances intracellular pH acidification. This possibility should be investigated further.

The confirmation that both snorkels and increased HP affect the TCA cycle, and that snorkels may to some extent compensate the negative effects of HP, is found when assessing the impact of HP alone. In high oil-degrading cultures equipped with snorkels (HPS vs. APS, Fig. S2B,D), the sole increase of HP decreased the transcript levels of TCA-cycle-related genes and increased those in the last conversion steps of acetyl-CoA to 2,3 butanediol (Fig. 5). In low oil-degrading cultures not equipped with snorkels (HPC vs. APC, Fig. S2B,D), transcript levels in the TCA cycle were comparable, but at increased HP transcript abundance in alternative routes for acetyl-CoA was higher (to $CO_2$, acetate and to dihydroxyacetone; Fig. S25).

Overall, this data indicates that snorkels can stimulate the oxidation of acetyl-CoA through the TCA cycle, thereby supporting hydrocarbons biodegradation in contaminated sediments. In anaerobic microorganisms, the standard electron transport chain for microbial respiration and ATP generation is highly branched, allowing the interaction of a broad range of electron donors and acceptors. The exact nature of such electron carriers inside the cell, how they relate to acetyl-CoA metabolism and to snorkels application must be clarified, but it may be hypothesized that they interact with sulfur metabolism (Marzocchi et al., 2020). Primary electron donors are both alkanes (Fig. S2D; Fig. S9-22) and aromatics (Fig. S2B; namely, via benzene, toluene, xylene and ciclohexane oxidation pathways; Figs. 6 and 1) which generate acetyl-CoA. As the negative impact of 10 MPa on the TCA cycle was here only partially compensated by snorkels, a new set-up should be tested to further stimulate these processes.

### 4.3. Snorkels shape sulfur metabolism at increased HP

Sulfur compounds were the main electron shuttles linking the intracellular reducing power generated by the cell to extracellular snorkels. Both assimilatory and dissimilatory $SO_4^{2-}$ reduction pathways eventually generate $H_2S$, which can leave the cell. The energy-consuming $SO_4^{2-}$ assimilatory pathway was much less expressed wrt the dissimilatory one across all treatments (Table S6,S9). Several sulfur compounds can be channeled into these two pathways and be reduced to $H_2S$ (e.g. $S_3O_6^{2-}$, $S_2O_3^{2-}$, $S_4O_6^{2-}$, Fig. 4). However, $H_2S$ accumulation in sediments was always offset by snorkels application wrt glass controls (Fig. S3C,D), with subsequent regeneration of $SO_4^{2-}$ (Fig. S3E,F). This maintained high levels of the main electron acceptor ($SO_4^{2-}$) while removing the product of anaerobic respiration ($H_2S$), possibly supporting the generation of more reducing power by the cell ultimately via hydrocarbons oxidation.

The sole increase of HP in the absence of snorkels (HPC vs. APC, Fig. S29) or the sole application of snorkels at ambient pressure (APS vs. APC, Fig. S30) did not alter sulfur metabolism transcript abundance. However, when both increased HP and snorkels presence/absence were considered together, a clear impact of snorkels emerged. For instance, the higher transcript abundance for several genes in sulfur metabolism at ambient wrt increased HP (APS vs. HPS; Fig. S24) reflects the fact that snorkels application could only partially compensate for the negative effects of increased HP. At increased HP, snorkels application (HPS vs. HPC) reduced the transcript abundance of the energy-consuming $SO_4^{2-}$ assimilatory pathways (Table S6A,B), a remarkable feature when cell homeostasis and energy balance are challenged (Scoma et al., 2016a, 2016b, 2018). Besides, snorkels application at increased HP led to a higher transcript abundance of genes related to the conversion of multiple sulfur compounds (i.e. $S_3O_6^{2-}$, $S_2O_3^{2-}$ and potentially alkanesulfonate, Fig. 4) into $SO_3^{2-}$. As transcript levels for the conversion of $SO_3^{2-}$ to $H_2S$ were also higher (Fig. 4), snorkels at increased HP (HPS) likely acted as electron sinks for a wider pool of sulfur compounds wrt HPC. These pathways involved the most represented bacterial taxa in sediments (*Deltaproteobacteria*, *Clostridia*, *Gammaproteobacteria*, Table S14). Overall, the positive impact of snorkels on both energy balance and diversity of sulfur-containing electron acceptors may have contributed to the enhanced alkane biodegradation in HPS wrt HPC (Fig. S2D). Last, the higher accumulation of $H_2S$ in HPC sediments wrt HPS (Fig. S3C) was consistent with the higher transcript abundance for polysulfide formation (Fig. 4). Surprisingly, the latter was not observed at ambient pressure (APS vs. APC, Fig. S30) despite a large difference in $H_2S$ accumulation (Fig. S2D), possibly because the lowest $H_2S$ levels in APS were however almost three times higher wrt HPS ($32.6 + 11.9$ vs. $13.3 \pm 2.7$ μM; Fig. S2D).

### 4.4. Sediment core community assemblage suggests a cross-talk between oil-degraders and sulfur oxidizers, while snorkels biofilms are selectively enriched in sulfur-oxidizing and often electroactive bacteria

The known core community members found in this study were either oil-degraders (*Dehalococcoidia* and *Fusibacter*) or chemolithoautotrophs (*Sulfurovum* and *Sulfurimonas*; Table S12A). The formers are found in the

most diverse hydrocarbon-contaminated environments (i.e. *Dehalococcoidia*, (Cheng et al., 2019; Hao et al., 2021; Karthikeyan et al., 2020; Pavlova et al., 2021; þorsteinsdóttir et al., 2020); *Fusibacter* (Agrawal et al., 2010; dos Santos et al., 2011; Hasegawa et al., 2014; Perez Calderon et al., 2019; Viggi et al., 2017; Wang et al., 2021)). The latter are also found in diverse oil-contaminated environments, but they are unable to use hydrocarbons directly; rather, they use $CO_2$ as carbon source and reduced sulfur species as electron donors (i.e. *Sulfurovum* (Lormieres and Oger, 2017; Marziah et al., 2016; Mu et al., 2021; Yeung et al., 2011); and *Sulfurimonas* (Kimak et al., 2019; Lormieres and Oger, 2017; Obi et al., 2017; Rubin-Blum et al., 2014; Tian et al., 2017; Watanabe et al., 2000; Yeung et al., 2011)). Irrespective of snorkels and HP effects, this confirms that sulfur species acted as electron shuttles in sediments between hydrocarbon-oxidizing, sulfur-reducing bacteria and sulfur-oxidizers.

Snorkels were selectively colonized by several species whose concentration was low in sediments, which together made up 17–35% of all the bacteria found on snorkel biofilms (Table 1; Table S13B,C). Irrespective of HP, a significant enrichment on snorkels biofilms was observed for *Draconibacterium* and *Desulfuromusa* (Table S13A). There is little information on *Draconibacterium* (Du et al., 2014), a facultatively anaerobic chemoorganotroph. It was enriched in the liquid phase of a bioelectrochemical reactor for anaerobic ammonium oxidation (Song et al., 2019) and in biofilms developed on biodegradable plastics (Denaro et al., 2020). *Desulfuromusa* (Liesak and Finster, 1994) uses several organic compounds to reduce sulfur and iron species (Liesak and Finster, 1994; Vandieken et al., 2006). It is an electroactive bacterium (Hnatush et al., 2019), and it has been enriched on graphite felt anodes treating wastewaters (Carmona-Martinez et al., 2015), and on anodes in sediment microbial fuel cells without (Holmes et al., 2004; Jung et al., 2014) and with hydrocarbons (particularly when spiking $Fe^{3+}$ (Hamdan and Salam, 2020)).

Increased HP specifically enriched snorkels biofilms in *Thiomicrorhabdus* and *Sulfitobacter* (Table S13B). *Thiomicrorhabdus* was introduced by (Boden et al., 2017), by reclassifying several *Thiomicrospira* species. It is an obligate chemolithoautotroph using $S_2O_3^{2-}$, $S_4O_6^{2-}$, $H_2S$ and, sometimes, $S^0$ as electron donors (but not thiocyanate [$SCN^-$], $SO_3^{2-}$, and Fe) and it fixes $CO_2$. Hence it may have been involved in cycling sulfur species on the snorkels surface. The heterotrophic *Sulfitobacter* was isolated at the $H_2S/O_2$ interface of the Black Sea (Sorokin, 1995), and was enriched on graphite (Erable et al., 2017), carbon cloth (Paitier et al., 2017) and stainless-steel anodes (De La Fuente et al., 2020), where it was inferred to either directly oxidize organic compounds, $SO_3^{2-}$ and/or $S_2O_3^{2-}$ (Erable et al., 2017; Paitier et al., 2017). Genes for aromatic hydrocarbons degradation were indeed found in the draft genome of two *Sulfitobacter* sp. (Mas-Llado et al., 2014), which is frequently enriched or abundant in oil-contaminated environments at ambient (Kostka et al., 2011; Krolicka et al., 2019; Marietou et al., 2018) and increased HP (22 MPa (Fasca et al., 2017)).

At ambient pressure, known genera selectively enriched on snorkel biofilms (Table S13C) were *Desulfoconvexum*, *Thioalkalispira* and *Sulfurimonas*. Little is known about *Desulfoconvexum* (Konneke et al., 2013), whose type species (*D. algidus*) is strictly anaerobic. Chemoorganotrophically, it can degrade fatty acids and aromatics to $CO_2$ while reducing either $SO_4^{2-}$, $S_2O_3^{2-}$ or $S^0$ to $H_2S$ (Konneke et al., 2013). Chemolithotropically, it uses $H_2$ as electron donor and $CO_2$ or bicarbonate as acceptors. *Thioalkalispira* (Sorokin, 2002) is an obligate chemolithoautotroph which can deposit intracellular sulfur globules. It can oxidize $H_2S$, polysulfide, $S^0$ and $S_2O_3^{2-}$ to $SO_4^{2-}$, it is considered an electrotroph which is recurrently found on cathodes (graphite felt (Zhu et al., 2021), granular activated carbon (Jugnia et al., 2021), carbon felt (Li et al., 2021) and stainless steel (Oldham et al., 2017)). Its presence on the anodic portion of the snorkel may have been related to its capacity to reduce $S^0$ to $H_2S$ (while not growing (Sorokin, 2002)). The facultatively anaerobic *Sulfurimonas* (introduced by (Inagaki et al., 2003); amended by (Takai et al., 2006)) grows chemolithoautotrophically with $H_2S$, $S^0$, $S_2O_3^{2-}$ and $H_2$ as electron donors using $NO_3^-$, $NO_2^-$ or $O_2$ as electron acceptors, and $CO_2$ as carbon source. It can corrode $Fe^0$ to $Fe_3(PO_4)_2$ when supplied with $H_2S$ and $NO_3^-$ as electron donor and acceptor (Lahme et al., 2019) and has been detected on graphite fiber brush anodes (Dai et al., 2020).

Overall, the microbial genera selectively enriched on snorkel biofilms were sulfur-oxidizing bacteria already known to colonize anodes, and often recognized as electroactive (e.g. *Desulfuromusa*, *Sulfitobacter*, *Thioalkalispira*).

### 4.5. Snorkels are not passivated by sulfur compounds, but increased HP facilitates the deposition of oxidized metals

No sulfur species was found to deposit on snorkels surface at either HP (Table 2). This indicates that oxidation of $H_2S$ on snorkels (Fig. S3A-D (Aulenta et al., 2021)) did not generate $S^0$ which could potentially reduce the snorkels available surface for further electroactive reactions, and it rather regenerated $SO_4^{2-}$, as indeed detected in bulk $SO_4^{2-}$ levels in the sediment pore water (Fig. S3E,F (Aulenta et al., 2021)). The selective enrichment of sulfur-oxidizing species on the snorkel biofilms suggests that such bacteria cooperated with snorkels' abiotic reactions to the full regeneration to $SO_4^{2-}$, e.g. via a potential $S^0$-scavenging activity on the snorkels surface.

However, at increased HP snorkels accumulated Al, Fe and P (Table 2). Accumulation of Fe species on electroactive snorkels applied to oil-contaminated sediments has been reported at ambient pressure (Viggi et al., 2015, 2017), but never specifically for increased HP.

In the present set up, $Fe^{2+}$ in the sediment pore water accumulated wrt $T_0$ at increased HP, while at ambient pressure $Fe^{2+}$ was equal or lower (Fig. S28). High $Fe^{2+}$ levels in the pore water at increased HP are thus consistent with Fe deposition only on snorkels at increased HP, where $Fe^{2+}$ can eventually be oxidized (abiotically) to $Fe^{3+}$ (Table 2). It remains unexplained why $Fe^{2+}$ levels in the pore water were HP-dependent. $Fe^{2+}$ can abiotically react with $H_2S$ to form FeS (AVS). In our set-up, $H_2S$ accumulation owing to hydrocarbons oxidation by $SO_4^{2-}$-reducing bacteria was indeed consistent with increasing AVS levels (Fig. S26). Besides, the lower $H_2S$ levels in snorkels treatments was consistent with lower AVS levels (Fig. S26). However, the high $Fe^{2+}$ levels at increased HP were unrelated to both snorkels presence (compare snorkels vs. controls, Fig. S28) and enhanced oil metabolism (compare alkane-poor vs. -rich crude oil, Fig. S28). This limits the relationship solely to increased HP and Fe metabolism, the exact mechanism of which should be investigated further.

## 5. Conclusions

Bioelectrochemical systems (i.e. snorkels) can enhance hydrocarbons oxidation at 10 MPa in piezosensitive communities collected from 0.1 MPa and affected by such a HP increase (Aulenta et al., 2021). Here, we show that: 1) increased HP impairs the TCA cycle and has no effect on transcript abundance and taxonomical composition in *beta* oxidation; 2) snorkels support the TCA cycle, thereby partially counterbalancing the negative effects of increased HP; 3) low oil-degrading cultures at increased HP and/or without snorkels show enhanced transcript abundance for pathways metabolizing acetyl-CoA via alternative routes to the TCA cycle (e.g. accumulation of intracellular carbon reserves); this suggests that high levels of acetyl-CoA and/or reduced electron carriers cannot be efficiently handled by these cells; 4) snorkels partially offset this limitation by stimulating the anaerobic respiration of hydrocarbons, e.g. via a larger pool of sulfur compounds used as intermediate electron acceptors, all using $H_2S$ as electron shuttle to the snorkel; 5) snorkels' biofilms are selectively enriched in sulfur-oxidizing, often electroactive bacteria, possibly contributing to scavenge all sulfur species on the snorkel's surface; 6) no passivation owing to sulfur cycling is observed on snorkels after seven weeks.

## Credit author statement

MB, Investigation, Data curation, Formal analysis, Writing - review & editing; EP, Investigation, Data curation; UM, Investigation, Writing - review & editing, Funding acquisition, Supervision; CCV, Investigation, Formal analysis; SR, Investigation, Formal analysis; FA, Conceptualization, Writing - review & editing; AS, Conceptualization; Data curation; Formal analysis; Funding acquisition; Investigation; Project administration; Supervision; Roles/Writing - original draft.

## Declaration of competing interest

The authors declare the following financial interests/personal relationships which may be considered as potential competing interests: Ugo Marzocchi reports financial support was provided by Grundfos Foundation.

## Acknowledgements

AS is in debt with Prof. Jo Philips (Aarhus University) and Dr. Katja Laufer-Meiser (Helmholtz Centre for Ocean Research Kiel) for their insights on iron metabolism and cycling. And with Prof. Kasper Urup Kjeldsen (Aarhus University) for his kind support with pressure reactors. UM was supported by the Grundfos Foundation (grant number 2017–025).

## Appendix A. Supplementary data

Supplementary data to this article can be found online at https://doi.org/10.1016/j.jenvman.2022.115244.

## References

Abe, F., 2007. Exploration of the effects of high hydrostatic pressure on microbial growth, physiology and survival: perspectives from piezophysiology. Biosci. Biotechnol. Biochem. 71, 2347–2357.
Abe, F., Horikoshi, K., 1998. Analysis of intracellular pH in the yeast Saccharomyces cerevisiae under elevated hydrostatic pressure: a study in baro- (piezo-) physiology. Extremophiles 2, 223–228.
Agrawal, A., Vanbroekhoven, K., Lal, B., 2010. Diversity of culturable sulfidogenic bacteria in two oil-water separation tanks in the north-eastern oil fields of India. Anaerobe 16, 12–18.
Andrews, S., 2010. FastQC. A Quality Control Tool for High Throughput Sequence Data, Babraham Bioinformatics. Babraham Institute, Cambridge.
Antipov, D., Bushmanova, E., Dvorkina, T., Gurevich, A., Kunyavskaya, O., Shlemov, A., Lapidus, A., Meleshko, D., Nurk, S., Prjibelski, A., Korobeynikov, A., 2019. SPAdes Family of Tools for Genome Assembly and Analysis (Poster).
Aulenta, F., Palma, E., Marzocchi, U., Cruz Viggi, C., Rossetti, S., Scoma, A., 2021. Enhanced hydrocarbons biodegradation at deep-sea hydrostatic pressure with microbial electrochemical snorkels. Catalysts 11.
Barbato, M., Scoma, A., 2020. Mild Hydrostatic-Pressure (15 MPa) Affects the Assembly, but Not the Growth, of Oil-Degrading Coastal Microbial Communities Tested under Limiting Conditions (5 Degrees C, No Added Nutrients). FEMS Microbiol Ecol.
Bartlett, D.H., 2002. Pressure effects on in vivo microbial processes. Biochim. Biophys. Acta 1595, 367–381.
Bartlett, D.H., Kato, C., Horikoshi, K., 1995. High pressure influences on gene and protein expression. Res. Microbiol. 146, 697–706.
Berg, J.M., Tymoczko, J.L., Gatto Jr., G.J., Stryer, L., 2015. Biochemistry, eighth ed. Freeman W.H. and Company, New York.
Boden, R., Scott, K.M., Williams, J., Russel, S., Antonen, K., Rae, A.W., Hutt, L.P., 2017. An evaluation of Thiomicrospira, Hydrogenovibrio and Thioalkalimicrobium: reclassification of four species of Thiomicrospira to each Thiomicrorhabdus gen. nov. and Hydrogenovibrio, and reclassification of all four species of Thioalkalimicrobium to Thiomicrospira. Int. J. Syst. Evol. Microbiol. 67, 1140–1151.
Bolger, A.M., Lohse, M., Usadel, B., 2014. Trimmomatic: a flexible trimmer for Illumina sequence data. Bioinformatics 30, 2114–2120.
Bushmanova, E., Antipov, D., Lapidus, A., Prjibelski, A.D., 2019. rnaSPAdes: a de novo transcriptome assembler and its application to RNA-Seq data. GigaScience 8.
Cantalapiedra, C.P., Hernandez-Plaza, A., Letunic, I., Bork, P., Huerta-Cepas, J., 2021. eggNOG-mapper v2: functional annotation, orthology assignments, and domain prediction at the Metagenomic scale. Mol. Biol. Evol. 38, 5825–5829.
Capece, M.C., Clark, E., Saleh, J.K., Halford, D., Heinl, N., Hoskins, S., Rothschild, L.J., 2013. Polyextremophiles and the constraints for terrestrial habitability. In: Seckbach, J., Oren, A., Stan-Lotter, H. (Eds.), Polyextremophiles. Life under Muliple Forms of Stress. Springer, pp. 3–60.
Carmona-Martinez, A.A., Trably, E., Milferstedt, K., Lacroix, R., Etcheverry, L., Bernet, N., 2015. Long-term continuous production of H2 in a microbial electrolysis cell (MEC) treating saline wastewater. Water Res. 81, 149–156.
Cheng, L., Shi, S.-b., Yang, L., Zhang, Y., Dolfing, J., Sun, Y.-g., Liu, L.-y., Li, Q., Tu, B., Dai, L.-r., Shi, Q., Zhang, H., 2019. Preferential degradation of long-chain alkyl substituted hydrocarbons in heavy oil under methanogenic conditions. Org. Geochem. 138.
Dai, Q., Zhang, S., Liu, H., Huang, J., Li, L., 2020. Sulfide-mediated azo dye degradation and microbial community analysis in a single-chamber air cathode microbial fuel cell. Bioelectrochemistry 131, 107349.
De La Fuente, M.J., Daille, L.K., De la Iglesia, R., Walczak, M., Armijo, F., Pizarro, G.E., Vargas, I.T., 2020. Electrochemical bacterial enrichment from natural seawater and its implications in biocorrosion of stainless-steel electrodes. Materials 13.
Denaro, R., Aulenta, F., Crisafi, F., Di Pippo, F., Cruz Viggi, C., Matturro, B., Tomei, P., Smedile, F., Martinelli, A., Di Lisio, V., Venezia, C., Rossetti, S., 2020. Marine hydrocarbon-degrading bacteria breakdown poly(ethylene terephthalate) (PET). Sci. Total Environ. 749, 141608.
Diomande, S.E., Nguyen-The, C., Guinebretiere, M.H., Broussolle, V., Brillard, J., 2015. Role of fatty acids in Bacillus environmental adaptation. Front. Microbiol. 6, 813.
dos Santos, H.F., Cury, J.C., do Carmo, F.L., dos Santos, A.L., Tiedje, J., van Elsas, J.D., Rosado, A.S., Peixoto, R.S., 2011. Mangrove bacterial diversity and the impact of oil contamination revealed by pyrosequencing: bacterial proxies for oil pollution. PLoS One 6, e16943.
Du, Z.J., Wang, Y., Dunlap, C., Rooney, A.P., Chen, G.J., 2014. Draconibacterium orientale gen. nov., sp. nov., isolated from two distinct marine environments, and proposal of Draconibacteriaceae fam. nov. Int. J. Syst. Evol. Microbiol. 64, 1690–1696.
Enns, T., Scholander, P.F., Bradstreet, E.D., 1965. Effect of hydrostatic pressure on gases dissolved in water. J. Phys. Chem. 69, 389–391.
Erable, B., Byrne, N., Etcheverry, L., Achouak, W., Bergel, A., 2017. Single medium microbial fuel cell: stainless steel and graphite electrode materials select bacterial communities resulting in opposite electrocatalytic activities. Int. J. Hydrogen Energy 42, 26059–26067.
Fasca, H., de Castilho, L.V.A., de Castilho, J.F.M., Pasqualino, I.P., Alvarez, V.M., de Azevedo Jurelevicius, D., Seldin, L., 2017. Response of marine bacteria to oil contamination and to high pressure and low temperature deep sea conditions. Microbiol. Open e550, 1–10.
Gontikaki, E., Potts, L.D., Anderson, J.A., Witte, U., 2018. Hydrocarbon-degrading bacteria in deep-water subarctic sediments (Faroe-Shetland Channel). J. Appl. Microbiol. 125, 1040–1053.
Hamdan, H.Z., Salam, D.A., 2020. Response of sediment microbial communities to crude oil contamination in marine sediment microbial fuel cells under ferric iron stimulation. Environ. Pollut. 263, 114658.
Hao, Z., Wang, Q., Yan, Z., Jiang, H., 2021. Novel magnetic loofah sponge biochar enhancing microbial responses for the remediation of polycyclic aromatic hydrocarbons-contaminated sediment. J. Hazard Mater. 401, 123859.
Hasegawa, R., Toyama, K., Miyanaga, K., Tanji, Y., 2014. Identification of crude-oil components and microorganisms that cause souring under anaerobic conditions. Appl. Microbiol. Biotechnol. 98, 1853–1861.
Holmes, D.E., Bond, D.R., O'Neil, R.A., Reimers, C.E., Tender, L.R., Lovley, D.R., 2004. Microbial communities associated with electrodes harvesting electricity from a variety of aquatic sediments. Microb. Ecol. 48, 178–190.
Huerta-Cepas, J., Szklarczyk, D., Heller, D., Hernandez-Plaza, A., Forslund, S.K., Cook, H., Mende, D.R., Letunic, I., Rattei, T., Jensen, L.J., von Mering, C., Bork, P., 2019. eggNOG 5.0: a hierarchical, functionally and phylogenetically annotated orthology resource based on 5090 organisms and 2502 viruses. Nucleic Acids Res. 47, D309–D314.
Inagaki, F., Takai, K., Kobayashi, H., Nealson, K.H., Horikoshi, K., 2003. Sulfurimonas autotrophica gen. nov., sp. nov., a novel sulfur-oxidizing epsilon-proteobacterium isolated from hydrothermal sediments in the Mid-Okinawa Trough. Int. J. Syst. Evol. Microbiol. 53, 1801–1805.
Ji, X.J., Huang, H., Ouyang, P.K., 2011. Microbial 2,3-butanediol production: a state-of-the-art review. Biotechnol. Adv. 29, 351–364.
Johansen, L., Bryn, K., Stormer, F.C., 1975. Physiological and biochemical role of the butanediol pathway in Aerobacter (Enterobacter) aerogenes. J. Bacteriol. 123, 1124–1130.
Joye, S.B., Teske, A.P., Kostka, J.E., 2014. Microbial dynamics following the macondo oil well blowout across gulf of Mexico environments. Bioscience 64, 766–777.
Jugnia, L.B., Manno, D., Vidales, A.G., Hrapovic, S., Tartakovsky, B., 2021. Selenite and selenate removal in a permeable flow-through bioelectrochemical barrier. J. Hazard Mater. 408, 124431.
Jung, S.P., Yoon, M.-H., Lee, S.-M., Oh, S.-E., Kang, H., Yang, J.-K., 2014. Power generation and anode bacterial community compositions of sediment fuel cells differing in anode materials and carbon sources. Int. J. Electrochem. Sci. 9.
Kanehisa, M., Sato, Y., Morishima, K., 2016. BlastKOALA and GhostKOALA: KEGG tools for functional characterization of genome and metagenome sequences. J. Mol. Biol. 428, 726–731.
Karthikeyan, S., Rodriguez, R.L., Heritier-Robbins, P., Hatt, J.K., Huettel, M., Kostka, J. E., Konstantinidis, K.T., 2020. Genome repository of oil systems: an interactive and searchable database that expands the catalogued diversity of crude oil-associated microbes. Environ. Microbiol. 22, 2094–2106.
Kato, C., Li, L., Nogi, Y., Nakamura, Y., Tamaoka, J., Horikoshi, K., 1998. Extremely barophilic bacteria isolated from the mariana trench, challenger deep, at a depth of 11,000 meters. Appl. Environ. Microbiol. 64, 1510–1513.

Kimak, C., Ntarlagiannis, D., Slater, L.D., Atekwana, E.A., Beaver, C.L., Rossbach, S., Porter, A., Ustra, A., 2019. Geophysical monitoring of hydrocarbon biodegradation in highly conductive environments. J. Geophys. Res.: Biogeosciences 124, 353–366.
Kimes, N.E., Callaghan, A.V., Suflita, J.M., Morris, P.J., 2014. Microbial transformation of the Deepwater Horizon oil spill-past, present, and future perspectives. Front. Microbiol. 5, 603.
King, G.M., Kostka, J.E., Hazen, T.C., Sobecky, P.A., 2015. Microbial responses to the Deepwater Horizon oil spill: from coastal wetlands to the deep sea. Ann. Rev. Mar. Sci 7, 377–401.
Konneke, M., Kuever, J., Galushko, A., Jorgensen, B.B., 2013. Desulfoconvexum algidum gen. nov., sp. nov., a psychrophilic sulfate-reducing bacterium isolated from a permanently cold marine sediment. Int. J. Syst. Evol. Microbiol. 63, 959–964.
Kopylova, E., Noe, L., Touzet, H., 2012. SortMeRNA: fast and accurate filtering of ribosomal RNAs in metatranscriptomic data. Bioinformatics 28, 3211–3217.
Korobeynikov, A., 2019. Tools for Assembly Graph Analysis via SPAdes Toolbox and More (Talk).
Kostka, J.E., Prakash, O., Overholt, W.A., Green, S.J., Freyer, G., Canion, A., Delgardio, J., Norton, N., Hazen, T.C., Huettel, M., 2011. Hydrocarbon-degrading bacteria and the bacterial community response in gulf of Mexico beach sands impacted by the deepwater horizon oil spill. Appl. Environ. Microbiol. 77, 7962–7974.
Krolicka, A., Boccadoro, C., Nilsen, M.M., Demir-Hilton, E., Birch, J., Preston, C., Scholin, C., Baussant, T., 2019. Identification of microbial key-indicators of oil contamination at sea through tracking of oil biotransformation: an Arctic field and laboratory study. Sci. Total Environ. 696, 133715.
Lahme, S., Enning, D., Callbeck, C.M., Menendez Vega, D., Curtis, T.P., Head, I.M., Hubert, C.R.J., 2019. Metabolites of an oil field sulfide-oxidizing, nitrate-reducing Sulfurimonas sp. cause severe corrosion. Appl. Environ. Microbiol. 85.
Li, Z.J., Jian, J., Wei, X.X., Shen, X.W., Chen, G.Q., 2010. Microbial production of meso-2,3-butanediol by metabolically engineered Escherichia coli under low oxygen condition. Appl. Microbiol. Biotechnol. 87, 2001–2009.
Li, X.M., Ding, L.J., Zhu, D., Zhu, Y.G., 2021. Long-Term fertilization shapes the putative electrotrophic microbial community in paddy soils revealed by microbial electrosynthesis systems. Environ. Sci. Technol. 55, 3430–3441.
Liesak, W., Finster, K., 1994. Phylogenetic analysis of five strains of gram-negative, obligately anaerobic, sulfur-reducing bacteria and description of desulfirornusa gen. Nov., including Desulfuromusa kysingii sp. nov., desulfurornusa bakii sp. nov., and Desulfuromusa succinoxidans sp. nov. Int. J. Syst. Bacteriol. 44, 753–758.
Lormieres, F., Oger, P.M., 2017. Epsilonproteobacteria dominate bacterial diversity at a natural tar seep. C R Biol. 340, 238–243.
Magee, R.J., Kosaric, N., 1987. The microbial production of 2,3-butanediol. Adv. Appl. Microbiol. 32, 89–161.
Mapelli, F., Scoma, A., Michoud, G., Aulenta, F., Boon, N., Borin, S., Kalogerakis, N., Daffonchio, D., 2017. Biotechnologies for marine oil spill cleanup: indissoluble ties with microorganisms. Trends Biotechnol. 35, 860–870.
Marietou, A., Chastain, R., Beulig, F., Scoma, A., Hazen, T.C., Bartlett, D.H., 2018. The effect of hydrostatic pressure on enrichments of hydrocarbon degrading microbes from the gulf of Mexico following the deepwater horizon oil spill. Front. Microbiol. 9, 808.
Marziah, Z., Mahdzir, A., Musa, M.N., Jaafar, A.B., Azhim, A., Hara, H., 2016. Abundance of sulfur-degrading bacteria in a benthic bacterial community of shallow sea sediment in the off-Terengganu coast of the South China Sea. Microbiologyopen 5, 967–978.
Marzocchi, U., Palma, E., Rossetti, S., Aulenta, F., Scoma, A., 2020. Parallel artificial and biological electric circuits power petroleum decontamination: the case of snorkel and cable bacteria. Water Res. 173, 115520.
Mas-Llado, M., Pina-Villalonga, J.M., Brunet-Galmes, I., Nogales, B., Bosch, R., 2014. Draft genome sequences of two isolates of the roseobacter group, sulfitobacter sp. strains 3SOLIMAR09 and 1FIGIMAR09, from harbors of Mallorca island (Mediterranean sea). Genome Announc. 2.
Matturro, B., Cruz Viggi, C., Aulenta, F., Rossetti, S., 2017. Cable bacteria and the bioelectrochemical snorkel: the natural and engineered facets playing a role in hydrocarbons degradation in marine sediments. Front. Microbiol. 8.
Mu, J., Leng, Q., Yang, G., Zhu, B., 2021. Anaerobic degradation of high-concentration polycyclic aromatic hydrocarbons (PAHs) in seawater sediments. Mar. Pollut. Bull. 167, 112294.
Nguyen, U.T., Lincoln, S.A., Valladares Juarez, A.G., Schedler, M., Macalady, J.L., Muller, R., Freeman, K.H., 2018. The influence of pressure on crude oil biodegradation in shallow and deep Gulf of Mexico sediments. PLoS One 13, e0199784.
NOAA/Hazardous Materials Response and Assessment Division Seattle, W., 1992. Oil Spill Case Histories, pp. 1–224.
Noirungsee, N., Hackbusch, S., Viamonte, J., Bubenheim, P., Liese, A., Muller, R., 2020. Influence of oil, dispersant, and pressure on microbial communities from the Gulf of Mexico. Sci. Rep. 10, 7079.
Obi, C.C., Adebusoye, S.A., Amund, O.O., Ugoji, E.O., Ilori, M.O., Hedman, C.J., Hickey, W.J., 2017. Structural dynamics of microbial communities in polycyclic aromatic hydrocarbon-contaminated tropical estuarine sediments undergoing simulated aerobic biotreatment. Appl. Microbiol. Biotechnol. 101, 4299–4314.
Oger, P.M., Jebbar, M., 2010. The many ways of coping with pressure. Res. Microbiol. 161, 799–809.
Oldham, A.L., Steinberg, M.K., Duncan, K.E., Makama, Z., Beech, I., 2017. Molecular methods resolve the bacterial composition of natural marine biofilms on galvanically coupled stainless steel cathodes. J. Ind. Microbiol. Biotechnol. 44, 167–180.
Paitier, A., Godain, A., Lyon, D., Haddour, N., Vogel, T.M., Monier, J.M., 2017. Microbial fuel cell anodic microbial population dynamics during MFC start-up. Biosens. Bioelectron. 92, 357–363.
Pavlova, O.N., Izosimova, O.N., Chernitsyna, S.M., Ivanov, V.G., Pogodaeva, T.V., Khabuev, A.V., Gorshkov, A.G., Zemskaya, T.I., 2021. Anaerobic oxidation of petroleum hydrocarbons in enrichment cultures from sediments of the Gorevoy Utes natural oil seep under methanogenic and sulfate-reducing conditions. Microb. Ecol. 83, 899–915.
Perez Calderon, L.J., Gontikaki, E., Potts, L.D., Shaw, S., Gallego, A., Anderson, J.A., Witte, U., 2019. Pressure and temperature effects on deep-sea hydrocarbon-degrading microbial communities in subarctic sediments. Microbiologyopen 8, e00768.
Potts, L.D., Perez Calderon, L.J., Gontikaki, E., Keith, L., Gubry-Rangin, C., Anderson, J. A., Witte, U., 2018. Effect of spatial origin and hydrocarbon composition on bacterial consortia community structure and hydrocarbon biodegradation rates. FEMS Microbiol. Ecol. 94.
Rho, M., Tang, H., Ye, Y., 2010. FragGeneScan: predicting genes in short and error-prone reads. Nucleic Acids Res. 38, e191.
Rubin-Blum, M., Antler, G., Turchyn, A.V., Tsadok, R., Goodman-Tchernov, B.N., Shemesh, E., Austin Jr., J.A., Coleman, D.F., Makovsky, Y., Sivan, O., Tchernov, D., 2014. Hydrocarbon-related microbial processes in the deep sediments of the eastern Mediterranean levantine basin. FEMS Microbiol. Ecol. 87, 780–796.
Scoma, A., 2021. Functional groups in microbial ecology: updated definitions of piezophiles as suggested by hydrostatic pressure dependence on temperature. ISME J. 15, 1871–1878.
Scoma, A., Barbato, M., Borin, S., Daffonchio, D., Boon, N., 2016a. An impaired metabolic response to hydrostatic pressure explains Alcanivorax borkumensis recorded distribution in the deep marine water column. Sci. Rep. 6, 31316.
Scoma, A., Barbato, M., Hernandez-Sanabria, E., Mapelli, F., Daffonchio, D., Borin, S., Boon, N., 2016b. Microbial oil-degradation under mild hydrostatic pressure (10 MPa): which pathways are impacted in piezosensitive hydrocarbonoclastic bacteria? Sci. Rep. 6, 23526.
Scoma, A., Yakimov, M.M., Boon, N., 2016c. Challenging oil bioremediation at deep-sea hydrostatic pressure. Front. Microbiol. 7.
Scoma, A., Heyer, R., Rifai, R., Dandyk, C., Marshall, I., Kerckhof, F.M., Marietou, A., Boshker, H.T.S., Meysman, F.J.R., Malmos, K.G., Vosegaard, T., Vermeir, P., Banat, I. M., Benndorf, D., Boon, N., 2018. Reduced TCA cycle rates at high hydrostatic pressure hinder hydrocarbon degradation and obligate oil degraders in natural, deep-sea microbial communities. ISME J. 13, 1004–1018.
Scoma, A., Garrido-Amador, P., Nielsen, S.D., Roy, H., Kjeldsen, K.U., 2019. The polyextremophilic bacterium Clostridium paradoxum attains piezophilic traits by modulating its energy metabolism and cell membrane composition. Appl. Environ. Microbiol. 85.
Seckbach, J., Oren, A., Stan-Lotter, H., 2013. Polyextremophiles - Life under Multiple Forms of Stress. Springer.
Simonato, F., Campanaro, S., Lauro, F.M., Vezzi, A., D'Angelo, M., Vitulo, N., Valle, G., Bartlett, D.H., 2006. Piezophilic adaptation: a genomic point of view. J. Biotechnol. 126, 11–25.
Song, Y.-C., Joicy, A., Jang, S.-H., 2019. Direct interspecies electron transfer in bulk solution significantly contributes to bioelectrochemical nitrogen removal. Int. J. Hydrogen Energy 44, 2180–2190.
Sorokin, D.Y., 1995. Sulfitobacter pontiacus gen. Nov., sp. nov.—a new heterotrophic bacterium from the Black Sea, specialized on sulfite oxidation. Mikrobiologiya 64, 354–365.
Sorokin, D.Y., 2002. Thioalkalispira microaerophila gen. nov., sp. nov., a novel lithoautotrophic, sulfur-oxidizing bacterium from a soda lake. Int. J. Syst. Evol. Microbiol. 52, 2175–2182.
Stookey, L.L., 1070. Ferrozine - a new spectrophotometric reagent for iron. Anal. Chem. 42, 779.
Takai, K., Suzuki, M., Nakagawa, S., Miyazaki, M., Suzuki, Y., Inagaki, F., Horikoshi, K., 2006. Sulfurimonas paralvinellae sp. nov., a novel mesophilic, hydrogen- and sulfur-oxidizing chemolithoautotroph within the Epsilonproteobacteria isolated from a deep-sea hydrothermal vent polychaete nest, reclassification of Thiomicrospira denitrificans as Sulfurimonas denitrificans comb. nov. and emended description of the genus Sulfurimonas. Int. J. Syst. Evol. Microbiol. 56, 1725–1733.
Tian, H., Gao, P., Chen, Z., Li, Y., Li, Y., Wang, Y., Zhou, J., Li, G., Ma, T., 2017. Compositions and abundances of sulfate-reducing and sulfur-oxidizing microorganisms in water-flooded petroleum reservoirs with different temperatures in China. Front. Microbiol. 8, 143.
Tsau, J.L., Guffanti, A.A., Montville, T.J., 1992. Conversion of pyruvate to acetoin helps to maintain pH homeostasis in lactobacillus plantarum. Appl. Environ. Microbiol. 58, 891–894.
Van Houdt, R., Aertsen, A., Michiels, C.W., 2007. Quorum-sensing-dependent switch to butanediol fermentation prevents lethal medium acidification in Aeromonas hydrophila AH-1N. Res. Microbiol. 158, 379–385.
Van Landuyt, J., Cimmino, L., Dumolin, C., Chatzigiannidou, I., Taveirne, F., Mattelin, V., Zhang, Y., Vandamme, P., Scoma, A., Williamson, A., Boon, N., 2020. Microbial enrichment, functional characterization and isolation from a cold seep yield piezotolerant obligate hydrocarbon degraders. FEMS Microbiol. Ecol. 96.
Vandieken, V., Mussmann, M., Niemann, H., Jorgensen, B.B., 2006. Desulfuromonas svalbardensis sp. nov. and Desulfuromusa ferrireducens sp. nov., psychrophilic, Fe (III)-reducing bacteria isolated from Arctic sediments, Svalbard. Int. J. Syst. Evol. Microbiol. 56, 1133–1139.
Viggi, C.C., Presta, E., Bellagamba, M., Kaciulis, S., Balijepalli, S.K., Zanaroli, G., Petrangeli Papini, M., Rossetti, S., Aulenta, F., 2015. The "Oil-Spill Snorkel": an

innovative bioelectrochemical approach to accelerate hydrocarbons biodegradation in marine sediments. Front. Microbiol. 6, 881.
Viggi, C.C., Matturro, B., Frascadore, E., Insogna, S., Mezzi, A., Kaciulis, S., Sherry, A., Mejeha, O.K., Head, I.M., Vaiopoulou, E., Rabaey, K., Rossetti, S., Aulenta, F., 2017. Bridging spatially segregated redox zones with a microbial electrochemical snorkel triggers biogeochemical cycles in oil-contaminated River Tyne (UK) sediments. Water Res. 127, 11–21.
Wang, M., Sha, C., Wu, J., Su, J., Wu, J., Wang, Q., Tan, J., Huang, S., 2021. Bacterial community response to petroleum contamination in brackish tidal marsh sediments in the Yangtze River Estuary, China. J. Environ. Sci. (China) 99, 160–167.
Watanabe, K., Watanabe, K., Kodama, Y., Syutsubo, K., Harayama, S., 2000. Molecular characterization of bacterial populations in petroleum-contaminated groundwater discharged from underground crude oil storage cavities. Appl. Environ. Microbiol. 66, 4803–4809.
Xiao, Z., Xu, P., 2007. Acetoin metabolism in bacteria. Crit. Rev. Microbiol. 33, 127–140.
Yayanos, A.A., 1995. Microbiology to 10,500 meters in the deep sea. Annu. Rev. Microbiol. 49, 777–805.
Yayanos, A.A., Dietz, A.S., Van Boxtel, R., 1979. Isolation of a deep sea barophilic bacterium and some of its growth characteristics. Science 205, 808–809.
Yeung, C.W., Law, B.A., Milligan, T.G., Lee, K., Whyte, L.G., Greer, C.W., 2011. Analysis of bacterial diversity and metals in produced water, seawater and sediments from an offshore oil and gas production platform. Mar. Pollut. Bull. 62, 2095–2105.
Yücel, M., Konovalov, S.K., Moore, T.S., Janzen, C.P., Luther, G.W., 2010. Sulfur speciation in the upper Black Sea sediments. Chem. Geol. 269, 364–375.
Zhu, G., Huang, S., Lu, Y., Gu, X., 2021. Simultaneous nitrification and denitrification in the bio-cathode of a multi-anode microbial fuel cell. Environ. Technol. 42, 1260–1270.
Þorsteinsdóttir, G.V., Blischke, A., Sigurbjornsdottir, M.A., Oskarsson, F., Arnarson Thorn, S., Magnusson, K.P., Vilhelmsson, O., 2020. Gas seepage pockmark microbiomes suggest the presence of sedimentary coal seams in the Oxarfjorethur graben of northeastern Iceland. Can. J. Microbiol. 66, 25–38.
Hnatush, S., Maslovska, O., Sehin, T., Vasyliv, O., Kovalchuk, M., Malovanyy, M., 2019. Waste water treatment by exoelectrogenic bacteria isolated from technogenically transformed lands. Ecol. Quest. 31.